The prehistoric and preindustrial deforestation of Europe

Jed O. Kaplan [a,b,*], Kristen M. Krumhardt [a], Niklaus Zimmermann [b]

[a] ARVE Group, Environmental Engineering Institute, Ecole Polytechnique Fédérale de Lausanne, Station 2, 1015 Lausanne, Switzerland
[b] Land Use Dynamics Unit, Swiss Federal Institute WSL, Zürcherstrasse 111, 9031 Birmensdorf, Switzerland

ARTICLE INFO

ABSTRACT

Humans have transformed Europe's landscapes since the establishment of the first agricultural societies in the mid-Holocene. The most important anthropogenic alteration of the natural environment was the clearing of forests to establish cropland and pasture, and the exploitation of forests for fuel wood and construction materials. While the archaeological and paleoecological record documents the time history of anthropogenic deforestation at numerous individual sites, to study the effect that prehistoric and preindustrial deforestation had on continental-scale carbon and water cycles we require spatially explicit maps of changing forest cover through time. Previous attempts to map preindustrial anthropogenic land use and land cover change addressed only the recent past, or relied on simplistic extrapolations of present day land use patterns to past conditions. In this study we created a very high resolution, annually resolved time series of anthropogenic deforestation in Europe over the past three millennia by 1) digitizing and synthesizing a database of population history for Europe and surrounding areas, 2) developing a model to simulate anthropogenic deforestation based on population density that handles technological progress, and 3) applying the database and model to a gridded dataset of land suitability for agriculture and pasture to simulate spatial and temporal trends in anthropogenic deforestation. Our model results provide reasonable estimations of deforestation in Europe when compared to historical accounts. We simulate extensive European deforestation at 1000 BC, implying that past attempts to quantify anthropogenic perturbation of the Holocene carbon cycle may have greatly underestimated early human impact on the climate system.

1. Introduction

Since the establishment of the first agricultural societies in Europe in the mid-Holocene (Price, 2000), humans have substantially altered the European landscape. The most evident and influential of these anthropogenic land cover and land use changes (LCLUC) has probably been the clearance of forests and woodlands for cropland and pasture and as a source of fuel wood and construction materials (Darby, 1956; Hughes and Thirgood, 1982). The rich paleoecological and archaeological record in Europe provides ample evidence that many European regions experienced intensive, continuous human occupation throughout the Holocene (e.g., Clark et al., 1989; Brewer et al., 2008; for a review see also Dearing, 2006). Indeed, some regions of Europe probably experienced successive cycles of deforestation, abandonment, and afforestation in the 6000 years of human history preceding the Industrial Revolution (e.g., Behre, 1988; Bintliff, 1993; Lagerås et al.,

1995; Berglund, 2000; Vermoere et al., 2000; Cordova and Lehman, 2005; Gaillard, 2007). This long history of anthropogenic activity had important implications for environmental change, from regional hydrology to possibly global climate, and contains lessons for our understanding of what constitutes environmental sustainability. In the current study, we attempt to estimate at high spatial and temporal resolution, the patterns of anthropogenic deforestation in Europe from the time agriculture was firmly established across the entire continent until the Industrial Revolution.

Though it is certain that the forests of many European countries were substantially cleared before the Industrial Revolution (in Europe, ca. 1790–1900), we lack a clear dataset describing the progression of deforestation that occurred during prehistoric and preindustrial times. The first studies that attempted to map the temporal pattern of anthropogenic land use and land cover change at the global to continental-scale before AD 1850 were limited in temporal extent to AD 1700 and relied on simplistic relationships between 20th century patterns of land use to extrapolate to earlier times (Ramankutty and Foley, 1999; Klein Goldewijk, 2001). constructed a contemporary permanent croplands map as a starting point for their model, and then ran a land cover change model backwards in time to the year 1700 using any available

* Corresponding author. Tel.: +41 21 693 8058; fax: +41 21 693 3913.
E-mail addresses: jed.kaplan@epfl.ch (J.O. Kaplan), kristen.krumhardt@epfl.ch (K.M. Krumhardt), niklaus.zimmermann@wsl.ch (N. Zimmermann).

historical cropland data as a constraint. This simple model used an algorithm for distributing cropland spatially over time, leaving country boundaries and other relics in the database.

The HYDE database of global historical land use change (Klein Goldewijk, 2001) was developed using population estimates as a proxy for the extent of agriculture over the past 300 years, including both cropland and pastureland. The starting point of this model was a spatially explicit global population map overlaid with country boundaries. Historical population records for each country were then used for temporal variation, while, using the assumption that high population density areas stay in the same place over time, spatial variation was provided by population distribution. Next, modern estimates of total cropland and pastureland per country were allocated back in time according to population density, with areas of higher population density being the first to be converted to cropland and pasture.

Most recently, Pongratz et al. (2008) synthesized a dataset of global LCLUC for the historical period (AD 800 – Present) that includes crop, pasture and natural land cover fractions. In this study, the authors referenced published maps of agricultural areas from the two studies described above (Ramankutty and Foley, 1999; Klein Goldewijk, 2001) as a starting point, then found the ratio of total land area used per capita for crop and pasture at AD 1700 for each country, and finally, using this ratio, scaled estimates of crop and pasture area by historical population estimates per country. This method is based on two major assumptions: 1) per capita land use for crop and pasture did not change prior to AD 1700, (though ranges provided in this dataset explicitly include uncertainties in estimates of past population and technological change), and 2) the spatial pattern of crop and pasture areas was exactly the same throughout the historical period as it was at AD 1700, i.e., the amount of land under cultivation in each gridcell at any given time is simply the AD 1700 value scaled by relative population change. In this way, the Pongratz et al. (2008) method propagates all uncertainties associated with the year AD 1700 land use maps in the Ramankutty and Foley (1999) and HYDE datasets (Klein Goldewijk, 2001).

In a global study assessing the effects of anthropogenic LCLUC since the mid-Holocene, Olofsson and Hickler (2007) also relied on the HYDE dataset of land cover change from AD 1700 onward. For four time slices prior to AD 1700, the authors used simple maps and literature on the spread of human civilization with historical world population records to estimate the extent of permanent and non-permanent agriculture since the mid-Holocene. As these references do not explicitly deal with land cover, all lands classified as being under "states and empires" were simply assumed to be 90% under agriculture, and a lower fraction of anthropogenic land use was assigned to areas occupied by "agricultural groups". The crude spatial and temporal resolution of this approach makes it unsuitable for anything more detailed than a global-scale assessment of human impact on the terrestrial biosphere on millennial time-scales. None of the currently available LCLUC datasets incorporate observations of land cover change from the historical record before AD 1700, or from paleoecological or archaeological data synthesis. Our new approach uses historical observations of land cover over the last two millennia to model the changing relationship between population and forest cover and overcome some of the limitations of previous datasets of prehistoric and preindustrial LCLUC.

It is likely that human modification of the environment, particularly through deforestation, would have had consequences for local to regional scale hydrology and climate, through changes in albedo, surface roughness and the balance of transpiration to runoff and groundwater recharge. A number of studies have demonstrated the sensitivity of regional climate to realistic levels of human impact (Eugster et al., 2000; Dümenil Gates and Ließ, 2001). In contrast, the effects of prehistoric and preindustrial

anthropogenic LCLUC on global climate are currently the subject of a lively debate (Ruddiman, 2007). Using a top down approach, a number of studies (Ruddiman et al., 2004; Vavrus et al., 2008) demonstrated the sensitivity of global climate to Holocene trends in atmospheric CO_2 and methane concentrations. As Ruddiman has argued (Ruddiman, 2005), these greenhouse gases could have had anthropogenic origins from deforestation resulting in CO_2 emissions, and the introduction of substantial populations of ruminant animals and development of rice agriculture, which increased methane emissions to the atmosphere. On the other hand, bottom up modeling studies that attempted to estimate prehistoric and preindustrial anthropogenic CO_2 emissions concluded that these emissions would have been too small to have had a substantial effect on global climate (DeFries et al., 1999; Olofsson and Hickler, 2007; Pongratz et al., 2009), and rather attribute the observed trends in CO_2 and methane concentrations to natural sources. However, given the limitations of these datasets described above, it is conceptually possible that they significantly underestimate anthropogenic emissions. Recently, a paleoecological data synthesis by Nevle and Bird (2008) concluded that afforestation after the collapse of populations in Latin America following European contact could have been significant enough to perturb the global carbon cycle and climate system.

In light of these confounding results and the limitations of current datasets, we attempt a new analysis of preindustrial and prehistoric anthropogenic LCLUC using updated datasets of historical population trends, climate and soils, and a novel method for inferring the relationship between population and land use based on observational forest cover data. Our goal is to quantify uncertainties in both population size and the rate of technological change and to estimate the sensitivity of our model to these driving variables. Our study focuses on Europe and neighboring regions because 1) this area has a record of human impact that covers the entire Holocene, 2) detailed estimates of historical population are available at national and sub-national level, and 3) the rich archaeological and paleoecological records enable us to make a least a qualitative evaluation of our model results.

2. Materials and methods

To estimate the deforestation of Europe, we developed a model of prehistoric and preindustrial LCLUC. The model is driven by human population size and constrained by suitability maps for agriculture and pasture, which are in turn based on gridded datasets of climate and soil properties. A relationship between population density and cleared area determines the amount of land that will be deforested by the human population at any given time. The suitability maps ensure that the most productive crop and pasturelands will be deforested first, with deforestation spreading to increasingly marginal land as population densities increase. A schematic of the deforestation model is presented in Fig. 1. Development and application of the deforestation model involved four steps: 1) assembling a spatially explicit database of human population from 1000 BC to AD 1850, 2) developing a relationship between population density and amount of cleared land, 3) preparing gridded maps of relative land suitability for crop and pasture and 4) combining these to create maps of forest cover.

2.1. Spatial and temporal domain

The spatial domain for our analysis is the area defined by the reference map projection and grid recommended by the EU INSPIRE Directive (Annoni et al., 2001; Annoni, 2005). This domain roughly covers Europe and neighboring areas from Iceland and Portugal to the Urals and from the Mediterranean to northernmost
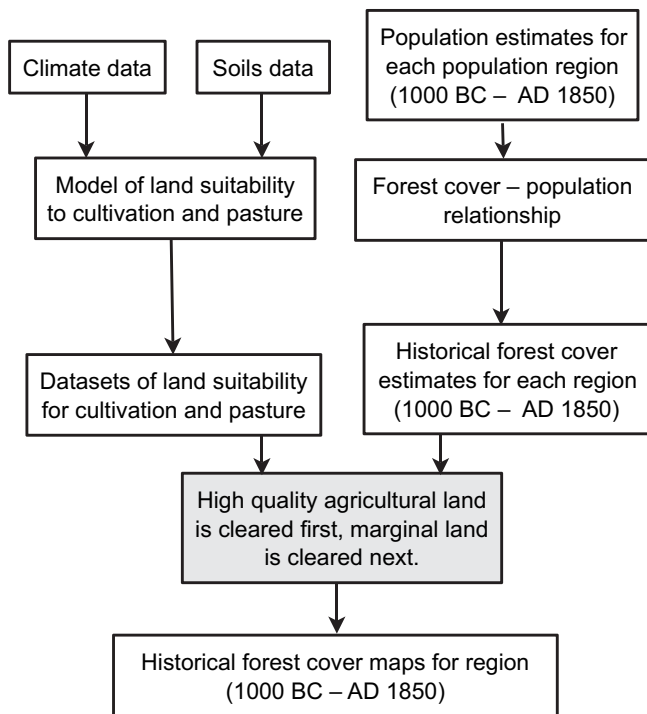
Fig. 1. Schematic of the preindustrial anthropogenic deforestation model, depicting the steps taken for spatial variability (left-hand side) and temporal variability (right-hand side) in order to generate historical land clearance maps of Europe.

Fennoscandia, covering part or all of more than 40 countries in Europe, North Africa and the Near East (Fig. 2). The temporal domain of our study covers the period 1000 BC to AD 1850. By 1000 BC, permanent agriculture was well-established everywhere in our spatial domain (Ammerman and Cavalli-Sforza, 1971; Price, 2000; Pinhasi et al., 2005), except for Iceland and the Faeroe Islands, and thus provides a reasonable starting point for our analysis that will not be complicated by the need to simulate the dispersal and establishment patterns of agricultural societies.

2.2. Historical population data

We developed a database of annually resolved population estimates from 1000 BC to AD 1850 for 52 regions of Europe, North Africa and the Near East (Fig. 2). Generally, one population region represents one country with the national boundaries of 1975, though in some cases, population regions are an amalgamation of countries, and in other cases, nations are divided into sub-regions. The population database is mainly based on the charts and spot estimates in McEvedy and Jones (1978), supplemented by other information where possible.

McEvedy and Jones (1978) contains continuous curves of total population for the period 400 BC to AD 1975 for a number of population regions covering the entire world. Curves for population regions in our study area were scanned and then rectified and digitized using GraphClick software (Arizona Software). To produce population estimates for the period prior to 400 BC, we extracted spot estimates for specific years from the text of McEvedy and Jones (1978), added these point estimates to the digitized data, and then linearly interpolated the data to produce estimates of annual population from 1000 BC to AD 1850.

Because McEvedy and Jones (1978) treat the whole of Russia-in-Europe as a single population region, we attempted to distribute the Russian population across this very large area by using

additional data sources. Lewis and Leasure (1966) provide estimates of the population of 12 major economic regions in European Russia for AD 1851. We distributed the total population of European Russia in AD 1850 from our McEvedy and Jones-based dataset according to the Lewis and Leasure (1966) estimate and scaled every prior year by the spatial distribution at AD 1850. While this simplification ignores, e.g., urban migration before AD 1851, we feel that the result is better than arbitrarily spreading the total population of European Russia over the entire area of the country, which would result in an unrealistic concentration of population in the southern, most agriculturally suitable part of European Russia (Chernozem belt). Similarly, to create population estimates for East Prussia, we obtained time slice estimates of population for several times in the past millennium (Jurkat, 2004), and reduced populations for Poland and the Russia West region accordingly.

The population estimates provided by McEvedy and Jones (1978), the main source of primary information for our database, have acknowledged uncertainties that increase with time into the past. To address these uncertainties and provide a model sensitivity test, we produced a range of alternative historical population estimates. Clark (1977) and Biraben (1979), provide estimates of population for Europe and the parts of North Africa and the Near East that are included in our spatial domain at selected time slices over the last three millennia. With these alternative estimates, we scaled the population within each region of our spatial domain to create continuous upper- and lower-bound estimates of population for the period 1000 BC to AD 1850.

In general, for earlier periods, McEvedy and Jones (1978) contained the most conservative, i.e., lower, population estimates, while in later periods they tended to be at the upper bound of estimations as compared to the other two references. The upper- and lower-bound time slice estimates of population for Europe and surrounding areas (our spatial domain) were linearly interpolated to create an annual time series, and then divided by the sum of estimates for all 52 population regions from McEvedy and Jones (1978) to produce a ratio for both the upper and lower boundaries. Subsequently, for each year and for each population region, upper- and lower-bound ratios were multiplied by the original population estimates from McEvedy and Jones (1978), to obtain annual upper- and lower-bound population estimates for each population region.

2.3. The relationship between population density and forest cover

In preindustrial societies, human population is the major driver of anthropogenic LCLUC (Darby, 1956; Mather et al., 1998b; Mather and Needle, 2000). As population density increases in a given area, the amount of land required to support this population will increase. Mather et al. (1998b) outlined two theoretical reasons for expecting a positive relationship between population and deforestation for preindustrial times. First, population growth stimulates the expansion of arable land for growing more food, which, in areas that would naturally be forested, generally results in deforestation. Secondly, a growing population means increased usage of forest products such as wood for fuel and construction materials, which can lead to an overall decline of forest area.

Population pressure on a landscape may be ameliorated by migration, trade and use of non-agricultural food resources (e.g., fishing), which may increase populations through external factors and by in situ improvements in the efficiency of the land base through technological innovation, development, and specialization. At a certain level of technological development, generally coinciding with industrialization and urbanization, most countries experience a "forest transition" where the relationship between population and the area of land under cultivation becomes
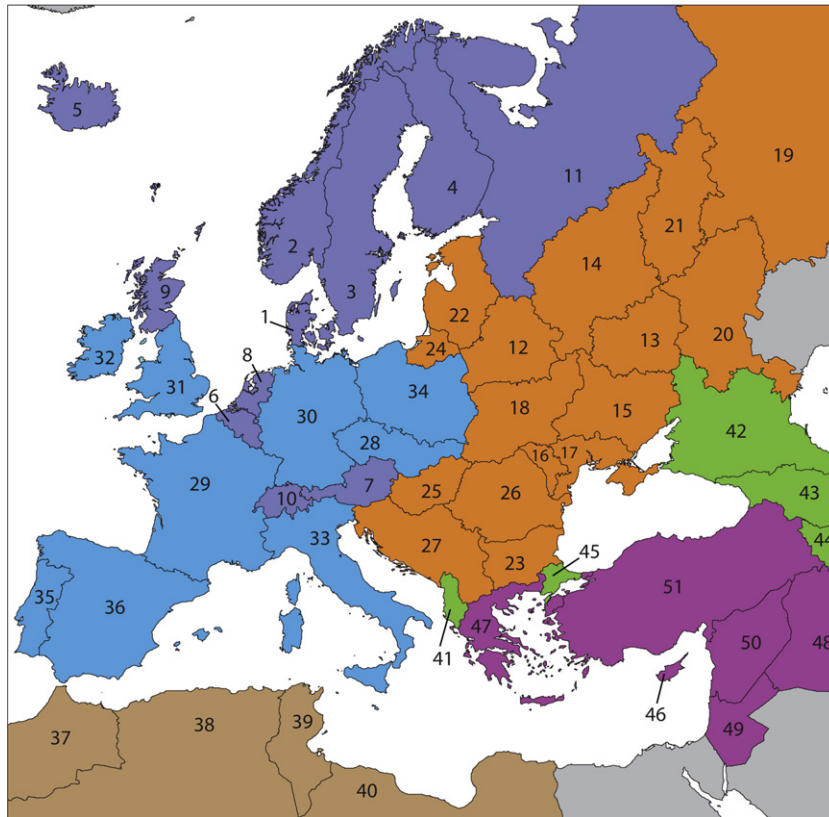
Fig. 2. Numbered map showing the population regions of our preindustrial anthropogenic deforestation model corresponding to the numbers listed for each region in Table 3. Regions with similar deforestation trends (see Fig. 8) throughout our study period are grouped using a certain color, while areas in gray ere not considered in this study.

uncoupled and in many cases even reverses, with afforestation concurrent with population growth (Mather, 1992, 2004; Rudel et al., 2005). Because the aim of this project is to develop a time series of deforestation prior to industrialization and therefore before forest transitions took place, and given that climate variability in Europe over the last 3000 years has been relatively small (Davis et al., 2003; Wanner et al., 2008), we assume that population change is the primary driver of changes in forest area for the years 1000 BC to 1850.

Mather (1999) proposes a sigmoidal log-linear relationship between population density and forest cover during the time preceding the forest transition, based on historical population and forest cover data from France. We expand on this approach by using data from other countries and building a relationship between population and forest cover to drive our model. Historical forest cover data was available for four European countries (Fig. 3a): Denmark, Ireland, France, and Sweden (Mather, 1999; Bradshaw, 2004). Among these historical forest cover data, the France data (Mather, 1999) is the most detailed and reliable because it is based on a wide variety of sources (e.g., historical records, statistical sources), but the other data is also valuable since it captures overall forest cover trends for diverse regions of Europe, necessary for building our generalized relationship. Since there are differences in the proportion of arable land and land productivity among countries, we needed to normalize both our population density and forest cover records to develop a population density-forest cover relationship that focuses on the key drivers in the relationship and eliminates country-specific biases.

2.3.1. Normalizing the population density axis

Historic agrarian societies tended to exist only where people could grow food, and therefore a better approximation of population density within a region is population density on the cultivatable land area (A_{crop}) within the population region (P_{dens}). Next, we needed to account for the quality of the usable land within a region. This was done by dividing the P_{dens} by the land suitability for cultivation on the usable land (S_{mean}), thus creating normalized population density (P_{norm}) (Table 2).

2.3.2. Normalizing the forest cover axis

In order to fit an inverse relationship between forest cover and population for preindustrial times, data for the years after the forest transition, where forest cover starts increasing with time (Fig. 3a), were eliminated from the forest cover datasets. Furthermore, because people typically cleared land to grow crops, create pastures, or use forest products, the forest cover estimates for each country were normalized by subtracting the unusable land (i.e., land that can not be used for crops, pasture, or that is generally uninhabitable by humans) from the potential maximum forest cover for each country. Therefore, the normalized dependent variable became forest cover only on usable land (FC_{norm}).

With both axes normalized, the time series of population density and forest cover for these four countries show a consistent relationship (Fig. 3b). Following Mather (1999), we build a "standard scenario" by fitting a sigmoidal curve to the FC_{norm} versus P_{norm} relationship using nonlinear least squares regression (R Development Core Team, 2005). The equation takes the form,

$$FC_{norm} = \frac{0.9958}{1 + e^{b(c - P_{norm})}}$$

(1)

where b and c are shape parameters that represent technological development and intensification.
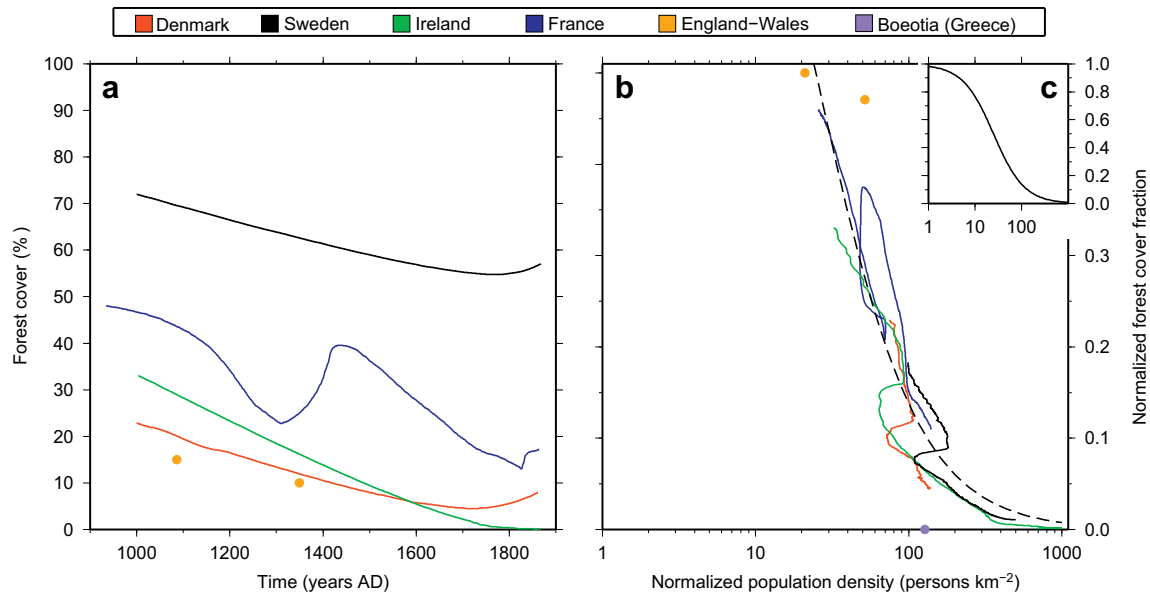
Fig. 3. Finding a relationship between forest cover and population. (a) Historical forest cover data for six European regions from Mather et al. (1999; France), Bradshaw (2004; Denmark, Sweden, and Ireland), Bintliff (1993; Boeotia) and Rackham and Rackham (1994; England–Wales). (b) Normalized population density (persons km^{-2} of cultivatable land/ S_{crop} of the cultivatable land) versus normalized forest cover fraction (forest cover on usable land). The dashed line represents the lower portion of a sigmoidal curve fit to the data for Denmark, Sweden, France, and Ireland, used for the standard scenario. Dots representing data for Boeotia and England–Wales are only used for our technology scenario. (c) Entire sigmoidal curve fit to the normalized data.

2.4. Technology and intensification

The population density-forest cover relationship was probably not constant over time. If a farmer can increase the number of people supported per unit area of land, then there is less pressure to clear forests and/or less suitable land can be abandoned. Therefore, major technological innovations in farming can result in changes of the relationship between population density and deforestation. In order to address this issue, we developed an alternative scenario for the population density-forest cover relationship over time. Using several additional data points for England–Wales originally from the Domesday Book (Rackham and Rackham, 1994), and the Boeotia region of central Greece (Bintliff, 1993), we fitted four distinct relationships between P_{norm} and FC_{norm} at certain time points of our model run: 350 BC, AD 1000, AD 1350, and AD 1830 (Fig. 4).

For each of the four time periods where estimates of forest cover were available (350 BC, AD 1000, AD 1350 and AD 1830), we adjusted the parameters of the sigmoidal fit curve to create four curves at fixed time slices that pass through the points on the graph representing this time in history. The changing shape of the curve between each time period represents technological evolution in the sense that as the curve shifts rightward, more people can be fed on the same amount of land. In our scenario including technological change, the model uses the appropriate relationship depending on the year of deforestation being calculated. For years between the fixed regression lines, we linearly interpolated the coefficients; at the beginning and end of the time domain of our study we held the coefficients constant to the earliest and latest fixed curves, respectively. Shape parameters of the sigmoidal curve for the standard scenario and the individual fixed time slices are presented in Table 1.

2.5. Estimating land suitability for crops and pasture

In order to make spatially explicit maps of LCLUC, it was necessary to devise a scheme for distributing human impact across the landscape. Following Ramankutty et al. (2002), we assumed

that in any given region the highest quality land for crops is cleared first, followed by increasingly marginal land for crop and pasture, as population pressure increases. For each $5' \times 5'$ gridcell in our spatial domain, we computed a fractional value for each of two indices: land suitability for cultivation (S_{crops}) and land suitability for pasture (S_{usable}).

We calculated S_{crops} as in Ramankutty et al. (2002), using climate and soil variables as the major constraints to cultivation. Climatic indicators to crop suitability were designated as growing degree days (GDD) and α, the ratio of actual evapotranspiration (AET) to potential evapotranspiration (PET). The indicators used for soil suitability were soil carbon density (C_{soil}) and the soil pH (pH$_{soil}$). Ramankutty et al. (2002) fitted suitability functions (based on locations of current croplands) to each of these four variables, the product of which is the index of land suitability to cultivation,

$$S_{crops} = f(GDD) \times f(\alpha) \times f(pH_{soil}) \times f(C_{soil}) \qquad (2)$$

Because plants generally grow everywhere that the climate allows, pasture suitability (S_{usable}) was calculated using only climatic variables, so that

$$S_{usable} = f(GDD) \times f(\alpha) \qquad (3)$$

In order to designate which gridcells could be used as pasture and which would remain undisturbed, we needed to assign a lower limit of S_{usable}. By evaluating present day and recent past distribution of crop/pasture lands and forests from various sources (Ramankutty and Foley, 1999; Klein Goldewijk, 2001; Päivinen et al., 2001), we found that any gridcell with a $S_{usable} > 0.075$ was "usable land". This cut-off point allowed us to explain the observed clearance, while providing a constraint to lands that do not have a climate hospitable enough to humans or domestic animals and therefore remained unchanged.

To calculate S_{crops} and S_{usable} we used high resolution ($5' \times 5'$) grids of 20th century climatology for temperature and precipitation (Hijmans et al., 2005) and fractional bright sunshine hours (New et al., 2002). To determine α, we calculated AET and PET following Prentice et al. (1993) and used high resolution gridded data of sand,
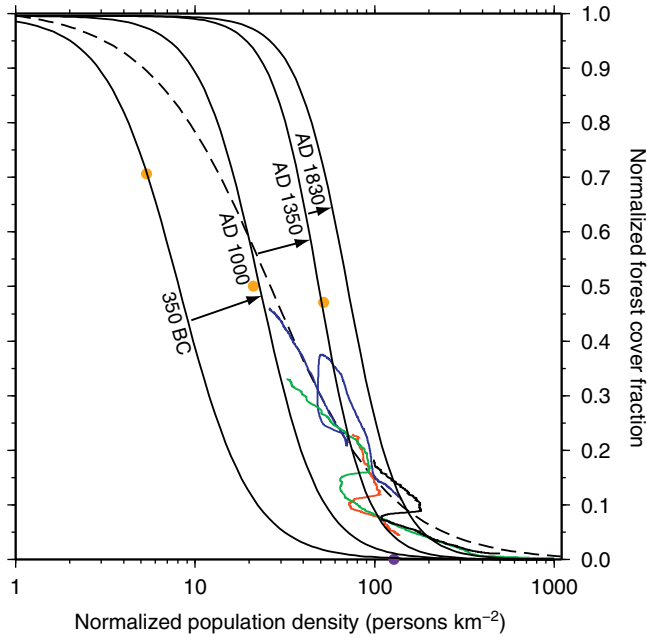
Fig. 4. Addressing technological progress in the relationship between population density and forest cover. Lines were fit to certain points in time for the data available. The line for year 350 BC is fit to two points: Boeotia at 400 BC (Bintliff, 1993) and the earliest data point for England–Wales at 300 BC (Rackham and Rackham, 1994). The AD 1000 line is fit to three points: the start points for the forest cover data for France and Ireland (AD 934 and AD 1003, respectively) (Mather 1999; Bradshaw, 2004), and the Domesday estimate for England–Wales at AD 1083 (Rackham and Rackham, 1994). The line for AD 1350, representing the Black Death event, is fitted for a forest cover estimate in England–Wales at the time of the Black Death (Rackham and Rackham, 1994) and the point on the France line where the distinct population drop due to the Black Death occurs (Mather 1999). Finally, the AD 1830 line is fitted to the last time point before the forest transition in France (Mather 1999) and Sweden (Bradshaw, 2004), and the last point of the Irish data (no forest transition occurred within the data) (Bradshaw, 2004). The arrows indicate the movement of the relationship with time. The dashed line is the population-forest cover relationship used in the standard scenario. Refer to Fig. 3 for color key.

clay, and organic matter content from the Harmonized World Soil Database (FAO/IIASA/ISRIC/ISSCAS/JRC, 2008) to calculate available soil water content following Saxon and Rawls (2006). The Harmonized World Soil Database also supplied data on C_{soil} and pH_{soil} for the top 30 cm of soil, the soil indicators used in the function to calculate S_{crops}.

2.6. Simulating anthropogenic deforestation

Using the datasets and model described above, we simulated annually resolved anthropogenic deforestation at 5′ resolution for the period 1000 BC to AD 1850 (Fig. 1). The modeling procedure had five parts (refer to Table 2 for variable definitions):

1. From the land suitability data, the summary statistics A_{crops}, A_{usable}, S_{mean}, and C_{frac} are calculated for each population region.

2. Year and population estimates are read in, calculating P_{dens} and P_{norm} for each population region at each time slice. FC_{norm} is then calculated according to Eq. (1).
3. DF_{frac}, the current cleared fraction of usable land, is calculated by subtracting FC_{norm} from one. If DF_{frac} becomes greater than or equal to C_{frac} with time, then the fraction of the gridcell used for growing crops is one and the remaining portion of DF_{frac} would then be designated as pasture, F_{usable}. F_{crops} cannot be larger than C_{frac}. However, if DF_{frac} is less than C_{frac}, then F_{crops} is simply the ratio of DF_{frac} to C_{frac}. This ratio will approach 1 as deforestation continues; i.e., if the cleared fraction of usable land is less than the amount of high quality cultivatable land, then the cleared fraction, DF_{frac}, will be 100% cropland and 0% pasture. As population density increases with time, DF_{frac} can become larger than C_{frac}, and lands of inferior quality are cleared for pasture.
4. The gridded variables, G_{crops} and G_{usable}, are computed for each time step. Within each gridcell of Europe, G_{crops} is calculated by multiplying the value of F_{crop} by the gridcell's crop suitability, S_{crops}, used here as the fractional value of the gridcell suitable for growing crops. G_{usable}, however, is calculated by multiplying F_{usable} by the difference of S_{crops} and S_{usable}. We must use the difference between S_{crops} and S_{usable} because here these two indices are used as fractional values, and S_{usable} will always include the fraction of land deemed as high quality cropland, C_{frac}.
5. The total anthropogenic land use of each gridcell, $G_{totalLU}$ is calculated by simply taking the sum of G_{crops} and G_{usable}.

Table 2
Abbreviations used for describing the preindustrial anthropogenic deforestation model.

Variable	Definition	Unit
Variables used to calculate S_{crops} and S_{usable}		
GDD	Growing degree days, an annual sum of daily mean temperatures over 5 °C	day °C
AET	Actual evapotranspiration, minimum of the evaporative demand and supply	mm h^{-1}
PET	Potential evapotranspiration, evaporative demand	mm h^{-1}
α	Moisture index; AET/PET	fraction
C_{soil}	Soil carbon density	kg C m^{-2}
pH_{soil}	Soil pH	pH scale
Input variables		
S_{crops}	Gridded dataset of land suitability for cultivation index	fraction
S_{usable}	Gridded dataset of land suitability for pasture index	fraction
P	Total population of a population region (annually, from 1000 BC to 1850)	persons
$A_{gridcell}$	Area of a gridcell (varies with latitude)	km^2
Constants for each population region		
A_{crops}	Area suitable for growing crops; $A_{gridcell} \times S_{crops}$	km^2
A_{usable}	Area that is suitable for pasture, i.e. usable; sum of $A_{gridcell}$ with a $S_{usable} > 0.075$	km^2
S_{mean}	Mean S_{crop} of usable land (where $S_{usable} > 0.075$)	fraction
C_{frac}	Fraction of the usable land suitable to grow crops	fraction
Variables for each population region		
P_{dens}	Population density on A_{crops}	persons km^{-2}
P_{norm}	Normalized population density, P_{dens}/S_{crops}	persons km^{-2}
FC_{norm}	Forest cover fraction of usable land	fraction
DF_{frac}	Cleared fraction of usable land, $1 - FC_{norm}$	fraction
F_{crops}	Fraction of cleared land used for crops	fraction
F_{usable}	Fraction of cleared land used for pasture (usable)	fraction
Gridded variables (model output)		
G_{crops}	Fraction of gridcell that is cropland; $F_{crops} \times S_{crops}$	fraction
G_{usable}	Fraction of gridcell that is pasture; $F_{usable} \times (S_{usable} - S_{crops})$	fraction
$G_{totalLU}$	Total land use (cleared) fraction of gridcell; $G_{crops} + G_{usable}$	fraction

Table 1
Values of shape parameters, b and c, for various curve fits of P_{norm} vs. FC_{norm} described by Eqn. (1), which vary in accordance to technological progress.

Curve	b	c
Standard scenario	−3.0	1.40
350 BC	−5.0	0.91
1000 AD	−6.0	1.36
1350	−7.5	1.69
1830	−7.0	1.85

3. Results

3.1. Land suitability for crops and pasture

Our simulation of land suitability for crops and pasture (Fig. 5) reveals that S_{crops} is markedly heterogeneous over the European landscape. This model, based on climate variables (GDD and α) and soil variables (pH$_{soil}$ and C_{soil}), shows the richest cultivation area to be the central band through the mid-latitudes of Europe (Fig. 5a). This central band is even more evident on the map of land suitability to pasture (S_{usable}), which was produced by a model constrained only by the climate variables GDD and α (Fig. 5b). Northern latitudes (the Nordic countries and northern Russian regions) of both maps are constrained by low temperatures, while southern latitudes (North African regions) are constrained by lack of water.

Land appears to be especially suited for cultivation in the regions bordering the Mediterranean Sea (excluding the desert coasts of Libya) and in the black earth region of the eastern European steppes. Soil characteristics put a constraint on S_{crops} in areas such as southwestern France and mid-southern Sweden. Central and southern Russian regions display consistently rich farmland, while central European soils are variable and broken up by mountain ranges such as the Alps, Pyrenees, and Carpathians. These high altitude regions are restrained by climate limitations and are thus deemed unusable by this model. Overall, the region of Europe, although variable in soil quality and topography, is rich in cultivatable land area and is suitable for pasture in most mid-latitude areas.

## 3.2. Historical forest cover estimates for the standard scenario

Historical forest cover estimates are presented in Fig. 8 and Table 3 as forested fractions of the usable land in each population region. Fig. 8 presents the time history of average forest cover in all of Europe and within six super-regions of Europe that showed similar trends in forest cover. Our standard scenario is presented in

blue and includes an area of error due to uncertainty in population estimations; the technology scenario is presented in red.

At the earliest time slice of our model, 1000 BC (Fig. 6, top left panel), the Near Eastern regions (Iraq, Syria-Lebanon, and Palestine-Jordan) clearly display widespread deforestation due to both the high population densities already achieved by that time and the low proportion of high quality agricultural land. Several small parts of central Europe (within Belgium, Switzerland, and Austria) display 70% clearance by 1000 BC, but overall the bulk of the European continent retains its forest cover in areas that were still mainly occupied by prehistoric societies. For example, North African and Eastern European regions display little or no deforestation at this time slice. In contrast, regions with very small amounts of cultivatable land such as Norway and Sweden had already cleared much of their usable land (a small area compared to the total area of the region) to be able to support their populations at this time (Table 3, Fig. 8).

Seven hundred years later, by 300 BC (Fig. 6, top right panel), forest clearance (agricultural areas) increased significantly in some parts of Europe and surrounding areas. The areas suited to agriculture within Greece, Algeria, and Tunisia, in particular, were classified as up to 90% under agriculture, while central and western European regions are calculated to have been between 10% and 60% deforested. Regions of the Near East continued to maintain their high population densities, while Eastern Europe, with low population densities, remained highly forested.

By AD 350 (Fig. 6, middle right panel), the collapse of the classical empires in Greece and neighboring regions led to lower population densities and afforestation in these areas relative to 300 BC. Central European regions, such as France, Germany, and Poland, showed moderately increased forest clearance (up to 90% in some areas) and Russian regions were just beginning to display significant levels of deforestation at this time. Although some regions exhibited a slight decrease in deforested area between AD 350 and AD 1000 (e.g., Central and Western Europe, see Fig. 8, group 3), net clearance of woodland in Europe did not change significantly (Fig. 6, middle panels). However, some regions that were previously
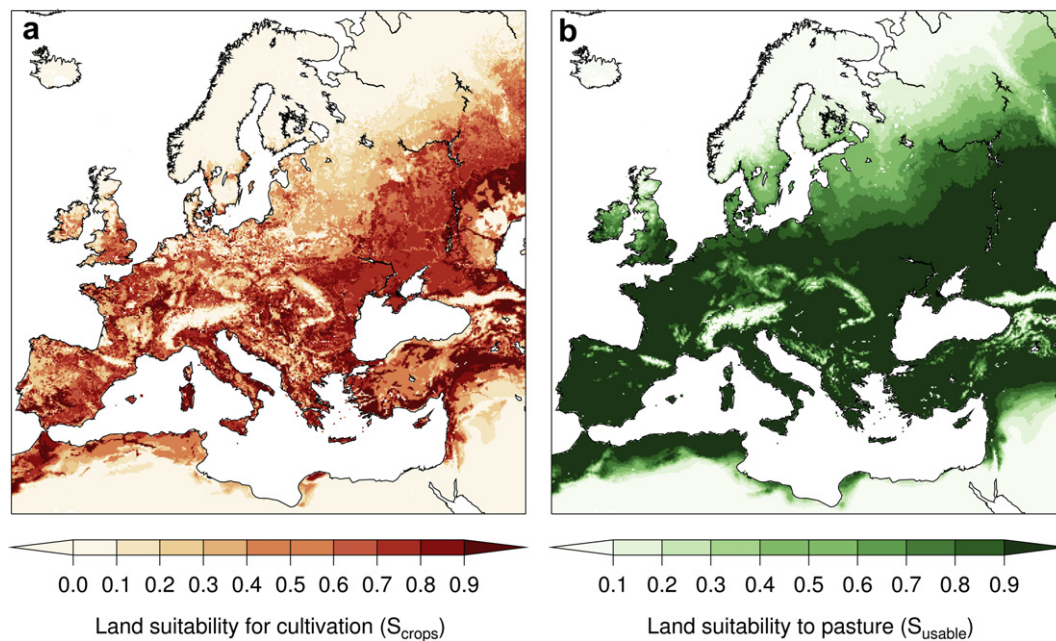
Fig. 5. Maps of land suitability for cultivation (a) and pasture (b). Land suitability to cultivation (S_{crops}) was simulated as in Ramankutty et al. (2002). Constraints to cultivation included both soil characteristics (soil pH, soil carbon density) from Harmonized World Soil Database (FAO/IIASA/ISRIC/ISSCAS/JRC, 2008) and climate data (air temperature, precipitation, and potential sunshine hours) from New et al. (2002) and Hijmans et al. (2005). Land suitability to pasture (S_{usable}) was constrained solely by the climate data.

Table 3
Numbered list of population regions corresponding to the map in Fig. 2 with estimates of percent usable land (land available for clearing for agriculture), and percent of forest cover on usable land by years 1000 BC, 500 BC, AD 1, AD 500, AD 1000, AD 1350, AD 1400, and AD 1850 for each region.

	% Forest cover on usable land:								
	Region	% Usable land	1000 BC	500 BC	AD 1	AD 500	AD 1000	AD 1350 (Black Death)	AD 1400	AD 1850
Northern & Alpine Europe										
1	Denmark	29.2	32.3	29.7	25.6	17.6	12.8	8.4	15.0	3.1
2	Norway	95.5	1.9	1.6	1.3	1.0	0.6	0.3	0.6	0.0
3	Sweden	79.8	27.1	24.2	17.7	13.8	9.9	4.8	8.8	0.7
4	Finland	86.7	67.8	65.1	17.0	8.5	5.4	4.2	3.0	0.0
5	Iceland	99.6	100.0	100.0	100.0	100.0	0.0	0.0	0.0	0.0
6	Belgium–Luxembourg	9.2	30.4	34.4	27.1	30.2	26.6	7.1	11.6	1.2
7	Austria	50.0	49.3	45.5	23.8	27.8	19.4	6.7	8.2	2.1
8	Netherlands	9.3	64.1	34.2	21.3	20.1	13.0	4.9	7.5	0.9
9	Scotland	72.9	12.5	6.8	7.2	4.8	2.8	0.7	1.3	0.1
10	Switzerland	58.1	41.8	20.8	18.0	18.9	17.6	5.0	9.1	1.3
11	Russia: Northwest	87.8	70.4	66.6	49.4	38.0	30.4	9.3	11.9	1.1
	Group 1 average	**48.0**	**45.2**	**39.0**	**28.0**	**25.5**	**12.6**	**4.7**	**7.0**	**1.0**
Eastern Europe										
12	Belarus	16.8	94.6	93.6	88.1	82.5	77.1	44.2	51.1	8.0
13	Russia: C. Chernozem	6.4	98.1	97.8	96.0	94.0	91.9	73.2	78.3	23.2
14	Russia: Central	32.1	92.2	90.8	83.1	75.7	69.1	34.3	40.8	5.4
15	Ukraine: East	1.7	98.9	98.8	98.0	97.0	96.0	85.9	88.9	40.6
16	Moldova	0.8	98.7	98.5	97.4	96.1	94.8	81.8	85.6	33.4
17	Ukraine: South	0.6	99.1	99.0	98.4	97.7	96.9	89.0	91.4	47.8
18	Ukraine: West	8.9	96.5	95.9	92.4	88.6	84.9	57.0	63.7	12.7
19	Russia: Ural	70.9	98.6	98.4	97.2	95.9	94.5	80.8	84.7	31.9
20	Russia: Volga	3.7	99.1	99.0	98.3	97.6	96.8	88.6	91.0	46.6
21	Russia: Volgo Viatsk	36.3	95.2	94.4	89.4	84.3	79.5	47.6	54.6	9.1
22	Baltics	35.1	93.0	91.8	84.8	77.9	71.7	37.2	43.9	6.1
23	Bulgaria	7.1	92.0	93.6	80.7	71.0	70.5	68.0	76.7	28.9
24	East Prussia	14.0	95.0	93.2	84.6	79.2	66.1	35.7	40.6	6.5
25	Hungary	0.6	85.9	84.3	85.3	89.8	73.2	42.2	52.3	14.3
26	Romania	11.5	83.1	82.6	82.1	87.1	83.4	62.2	70.9	17.5
27	Yugoslavia	9.4	85.0	75.2	61.2	56.9	55.6	41.1	54.4	19.4
	Group 2 average	**16.0**	**94.1**	**92.9**	**88.6**	**85.7**	**81.4**	**60.5**	**66.8**	**22.0**
Central & Western Europe										
28	Czechoslovakia	23.0	76.0	65.2	37.5	43.6	31.3	12.7	16.3	3.2
29	France	7.4	78.8	72.1	46.5	50.3	38.6	16.2	23.9	6.3
30	Germany	14.3	71.8	64.1	35.0	32.9	29.1	9.9	15.0	3.0
31	England-Wales	20.1	90.0	86.1	59.4	64.1	39.6	12.4	17.1	1.9
32	Ireland	30.0	64.5	68.4	69.7	50.6	38.0	13.0	19.0	0.9
33	Italy	10.4	69.0	51.1	30.1	47.9	40.2	22.1	30.0	7.6
34	Poland	9.9	95.0	91.1	75.1	69.9	46.1	22.2	24.8	4.0
35	Portugal	0.6	73.5	68.2	51.3	54.4	42.9	21.1	32.9	7.0
36	Spain	4.4	75.9	68.9	52.1	57.8	56.0	37.7	44.9	18.5
	Group 3 average	**13.3**	**77.2**	**70.6**	**50.7**	**52.4**	**40.2**	**18.6**	**24.9**	**5.8**
North Africa										
37	Morocco	40.6	98.0	88.4	67.8	69.6	49.5	43.4	55.8	31.7
38	Algeria	89.1	93.5	65.7	29.1	45.4	27.4	26.1	36.7	17.4
39	Tunisia	56.9	85.3	49.8	19.8	24.0	19.0	19.0	25.8	15.7
40	Libya	96.4	98.9	98.9	16.4	35.5	15.5	27.6	21.6	15.2
	Group 4 average	**70.7**	**93.9**	**75.7**	**33.3**	**43.6**	**27.8**	**29.0**	**35.0**	**20.0**
Eastern Regions with consistently high forest cover										
41	Albania	8.0	79.5	71.1	69.9	67.0	66.5	64.4	63.7	40.7
42	Russia: Ciscaucus	9.1	99.3	99.1	99.1	98.9	98.5	95.8	96.6	84.4
43	Transcaucasia	25.4	94.1	91.3	93.1	90.7	88.5	71.5	76.5	45.0
44	Iran	58.0	81.1	64.8	64.1	58.8	59.8	68.1	69.5	44.2
45	Turkey-in-Europe	0.4	96.5	93.2	91.1	66.2	65.3	65.0	65.0	37.6
	Group 5 average	**20.2**	**90.1**	**83.9**	**83.5**	**76.3**	**75.7**	**73.0**	**74.3**	**50.4**
Eastern Regions with consistently low forest cover										
46	Cyprus	5.1	75.6	60.4	40.3	43.4	41.9	43.6	47.3	47.2
47	Greece	2.2	58.3	33.1	45.9	67.1	67.0	59.7	73.8	32.0
48	Iraq	62.2	15.7	16.8	19.3	17.3	8.8	19.1	19.3	15.0
49	Palestine-Jordan	75.1	21.2	29.1	12.4	26.6	19.2	15.3	22.4	16.6
50	Syria-Lebanon	32.8	47.0	32.0	18.0	28.4	28.5	27.0	30.5	24.4
51	Turkey-in-Asia	9.4	74.5	71.2	59.1	63.4	53.9	58.2	63.3	42.2
	Group 6 average	**31.1**	**48.7**	**40.4**	**32.5**	**41.0**	**36.5**	**37.1**	**42.8**	**29.6**
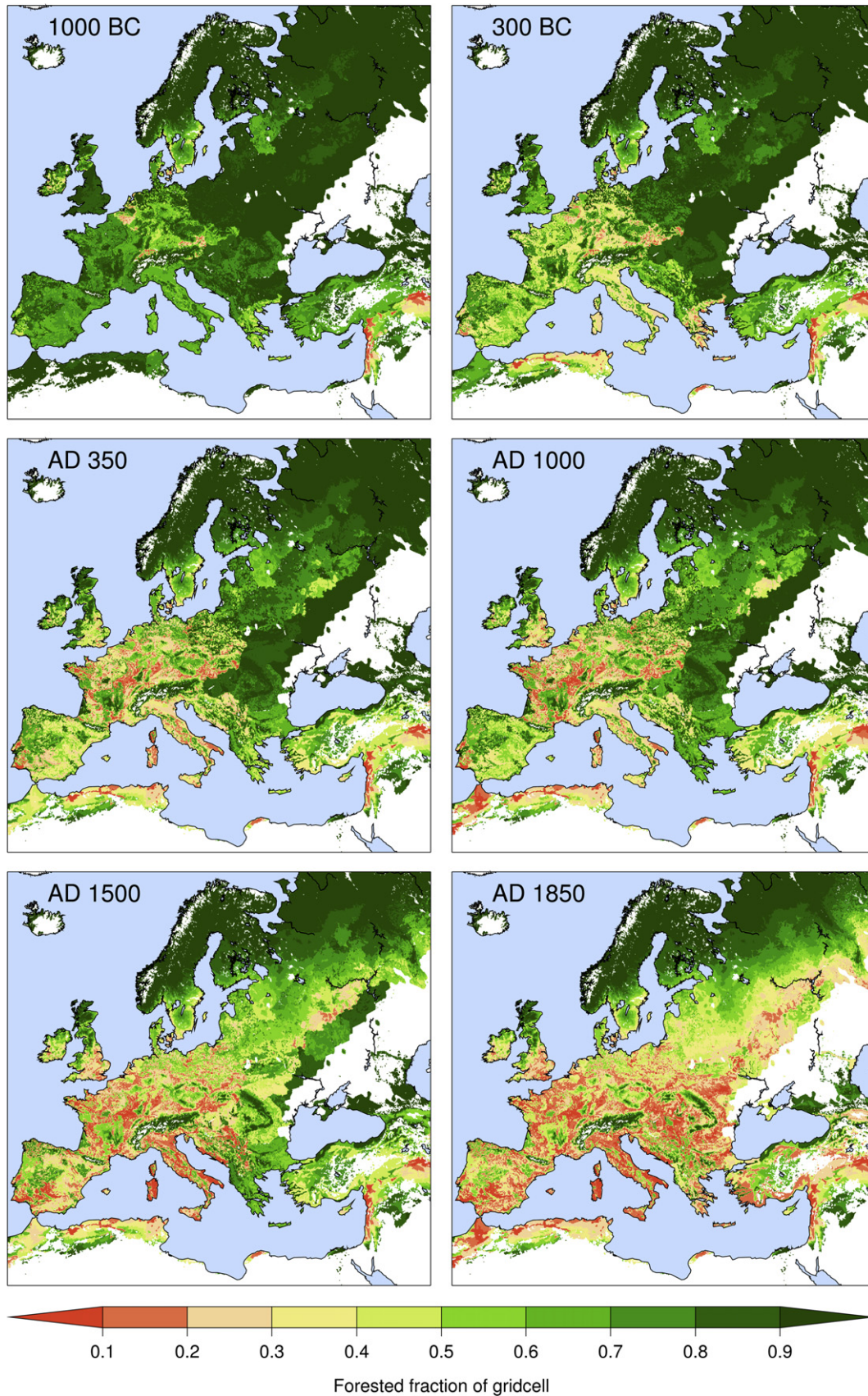
Fig. 6. Historical forest clearance maps for 1000 BC, 300 BC, AD 350, AD 1000, AD 1500, and AD 1850 as generated by the preindustrial anthropogenic deforestation model. Areas classified by Ramankutty and Foley (1999) as Savanna, Grassland/Steppe, Tundra, Desert, Polar Desert/Rock/Ice, or Open Shrubland with an $S_{usable} < 0.1$ are not considered forest and are left white.

highly deforested (e.g., Greece) displayed a continued increase in forest cover.

For many regions of Europe after AD 1000, deforestation continued steadily until the period of the Black Death, around AD 1350 (Fig. 8; Table 3). The major decline in population caused by this epidemic was reflected in the widespread afforestation of many regions of Europe, and was noticeable by AD 1400. Nearly all regions displayed either a pause in deforestation or an increase in forest area (Table 3). Regions with very low amounts of usable land showed no reforestation (e.g., Iceland). Populations of most regions of Europe had recovered to their pre-plague levels by AD 1450, and thus clearance levels were similar to those just prior to the Black Death. Consequently, from AD 1500 to AD 1850, we see the highest rates of forest clearance in our dataset and most usable land in Europe and surrounding regions became highly cleared just prior to industrialization. Notably during this period, Eastern Europe clearly displayed a steep rise in deforestation for the first time in history (e.g., Romania and Bulgaria, see Table 3 and Fig. 6, lower panels).

3.3. Technological change scenario

In our scenarios that include technological change, with increasing efficiency of land use over time, deforestation levels were greater than in the standard scenario for the first half of our study period and reduced in the second half (Fig. 7 as compared to Fig. 6). At 1000 BC, forested area is much more reduced in our technology scenario than in the standard scenario because people had less advanced techniques and needed to clear more forest to produce enough food to feed the populations during this early epoch. As time progresses, technology improved but populations became denser, thus creating a balance and little change in cleared area becomes apparent in our deforestation maps (Fig. 7). However, some countries became more forested due to technological developments during the later times of our model run, the most obvious of these being Spain, Morocco, Greece, and Turkey. These regions seem to have had low enough population densities that, when incorporating technological improvements, they could let previously cleared marginal lands return to forest and woodland, while still producing enough food to support their populations.

3.4. Historical trends in deforestation

The overall trend in LCLUC over our time domain is a constant decline in forest cover, interrupted by two local maxima: at AD 600, during the transition from Late Antiquity to the Early Middle Ages, and at AD 1400 shortly after the Black Death (Fig. 8; Table 3). Uncertainty in our population estimates tends to result in greater deforestation during earlier times as compared to our standard scenario, which has relatively conservative estimates of population for most regions. However, the effects of technological change, apparent in our technology scenario, are much greater than the effects of uncertainty in population estimates and indicate that the greatest periods of deforestation in much of Europe may have occurred already in the 14th century (Fig. 8). In order to better understand the time series of anthropogenic deforestation produced by our model, it is instructive to separate the whole of our spatial domain into groups of population regions that share similar trends and have similar geographic, environmental and/or historic settings. For example, Alpine Europe fits with Northern Europe because these Western European regions both have relatively low fractions of usable land. The super-regions used in the following analysis are identified with distinct colors in Fig. 2.

In the population regions of northern and Alpine Europe most of the usable land is deforested throughout the time domain of our model simulations (Fig. 8, group 1). This group includes northern regions with historically high population densities (e.g., Belgium–Luxembourg and the Netherlands), as well as regions with low amounts of usable land (e.g., all of the Nordic countries). Switzerland and Austria are also included in this group, as they have relatively small proportions of usable land due to the mountainous terrain and high population densities. The usable land of Iceland, which was unpopulated until the 9th century, is almost instantaneously deforested at the time of the arrival of the first permanent settlers because most of this region is deemed unsuitable for either crops or pasture.

In contrast to northern and Alpine Europe, Eastern Europe experiences relatively low amounts of deforestation for most of the time domain (Fig. 8, group 2). This group, which includes Yugoslavia, Bulgaria, Romania, Hungary, East Prussia, the Baltics, and most of the Russian regions, displayed relatively low forest clearance compared to other regions of Europe. Low population densities and relatively good suitability for crops and pasture meant that the large fraction of usable land in these regions was not heavily exploited until the final century of the time series. Central and western Europe (Fig. 8, group 3) also have largely high suitability for crops and pasture, but due to these regions' much greater population densities as compared to regions farther east, deforestation is significant throughout the model run. Important periods of afforestation occur during the "Migration Period" after the collapse of the Western Roman Empire (Halsall, 2007), and immediately following the Black Death in the 14th century.

Maghreb regions of North Africa display a distinct pattern of low clearance during early times with a relatively rapid increase in deforestation at around 200 BC (Fig. 8, group 4). The remaining Near East, Balkan, and Caucasian regions can be broken into two main groups: those with consistently high forest cover over time (e.g., Caucasus and Iran) and those with consistently low forest cover throughout the model run (e.g., Palestine-Jordan and Iraq) (Fig. 8, groups 5 and 6). These regions with high forest clearance, in particular, had high population densities even at 1000 BC and maintained a fluctuating but constant human presence throughout the Holocene (McEvedy and Jones, 1978).

The effects of our technological progress scenario on deforestation in the regional super-groups are displayed in the red lines on Fig. 8. For northern and Alpine Europe, the small amount of usable land available in these regions stays nearly 100% cleared throughout history when incorporating technology. For most other regions of Europe and surrounding areas, we observe greater deforestation in early times and a larger magnitude of afforestation after depopulating events (e.g., collapse of empires, war, plague). Nevertheless, each region shows a unique trend when technological advancement interacts with the individual characteristics (crop and pasture suitability, amount of usable land, population history) of each region in our model (Fig. 8, red lines).

3.5. Relationships between land quality and population density

Our preindustrial anthropogenic deforestation model is also useful in showing a relationship between land quality (i.e., S_{crop}) and the amount of people supported per unit area of land cleared for agriculture. Fig. 9 shows the progression of this relationship for several time slices of our standard scenario model simulation. Aside from Iceland, the relationship is simple and obvious for most regions of our study area during the first 2000 years of our model run: more people can be supported per km^2 in regions that have higher suitability for crops and pasture than in regions with a lower proportion of quality land (Fig. 9, top panels). As time progresses, this relationship becomes less distinct and by AD 1500 several European countries (most notably Belgium–Luxembourg, Austria, and Switzerland) begin to diverge from the relationship (Fig. 9,
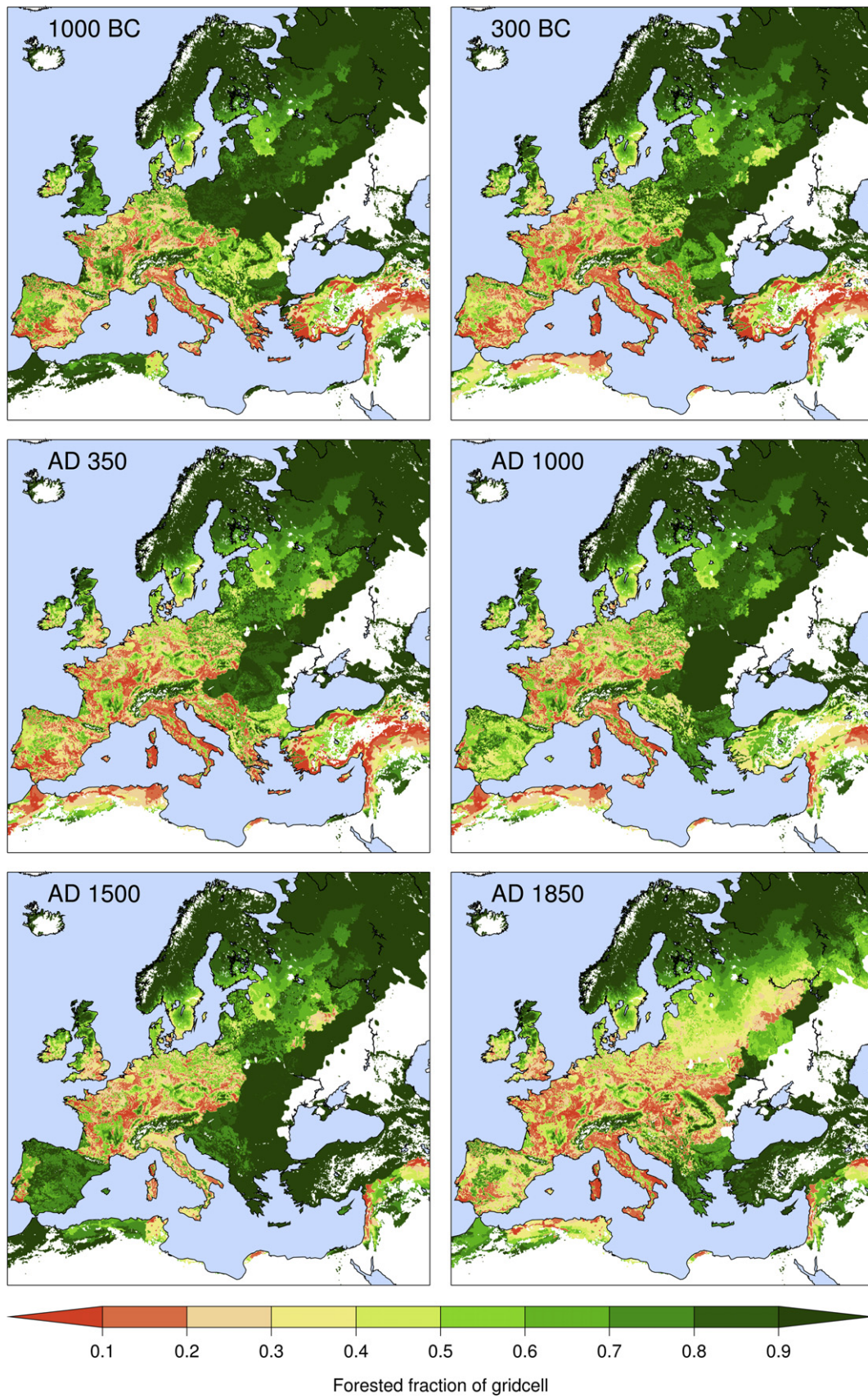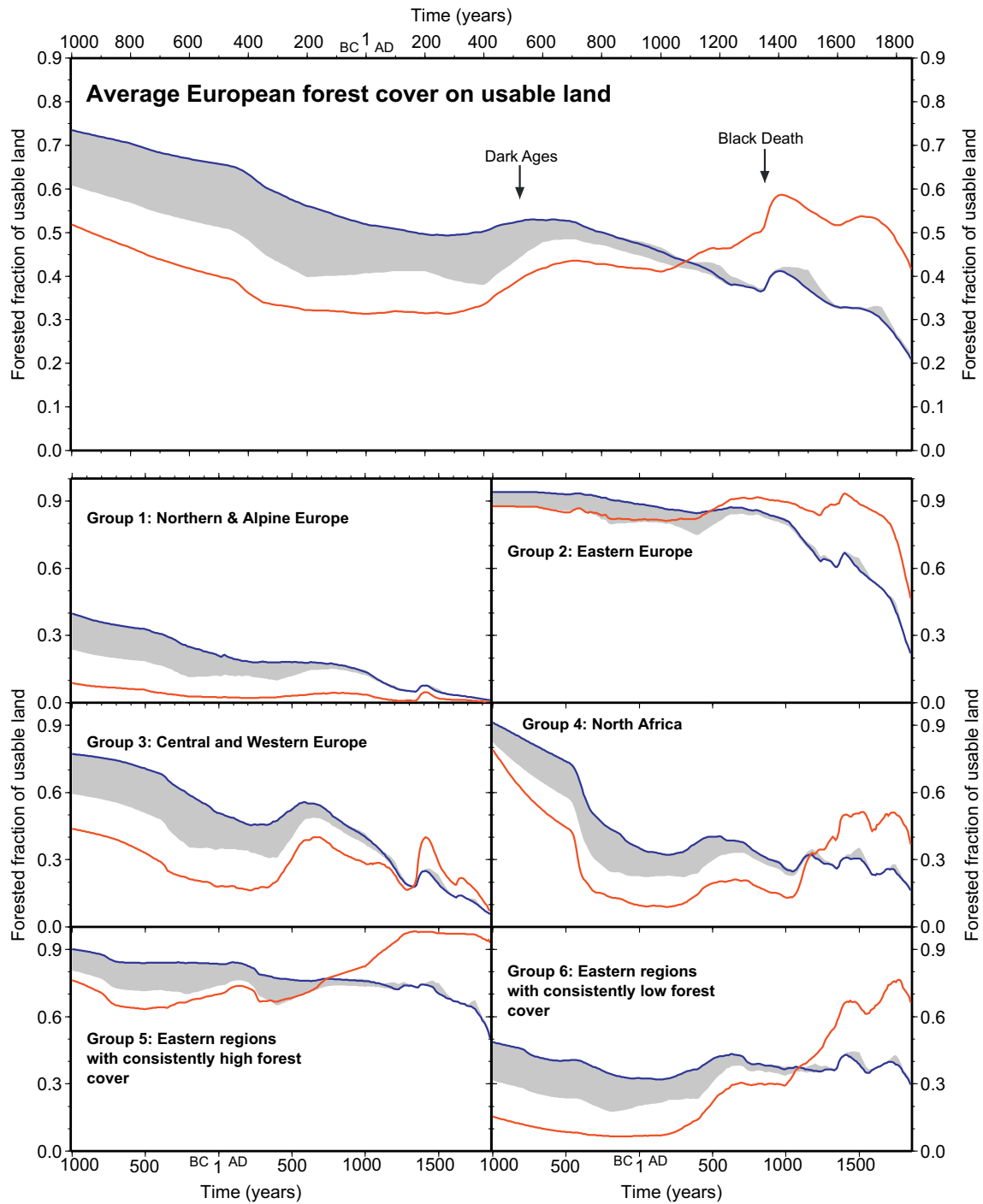
Fig. 7. Historical forest clearance maps generated by the technological change scenario version of the preindustrial anthropogenic deforestation model with the same presentation as in Fig. 6.

Fig. 8. Time versus deforested fraction of usable land for all of Europe and groups of population regions that displayed similar deforestation trends. Deforestation generated from population data from McEvedy and Jones (1978) is represented by the blue line, while gray area represents deforestation generated by a range of available population estimates for our study period. The red line represents the deforestation of each group under the technological change scenario. (For interpretation of the references to color in this figure legend, the reader is referred to the web version of this article.)

lower left panel). The relationship is nearly unrecognizable by AD 1850 as many regions increase the amount of people fed relative to their land suitability for agriculture. When determining the carrying capacity of each region for more recent times, it becomes clear that beyond land quality, factors such as industrialization, urbanization, trade, and exploitation of food resources other than agriculture become important. In the following discussion, we will attempt to explain how these trends may have affected the forest cover of Europe over the last three millennia.

4. Discussion

4.1. Land suitability for crops and pasture

By observing the general allocation of modern croplands (Päivinen et al., 2001) the gridded dataset produced by the land suitability for cultivation model (Ramankutty and Foley, 1999) is a viable estimation of the distribution of fertile cropland within Europe. Nevertheless, developing another less constrained gridded
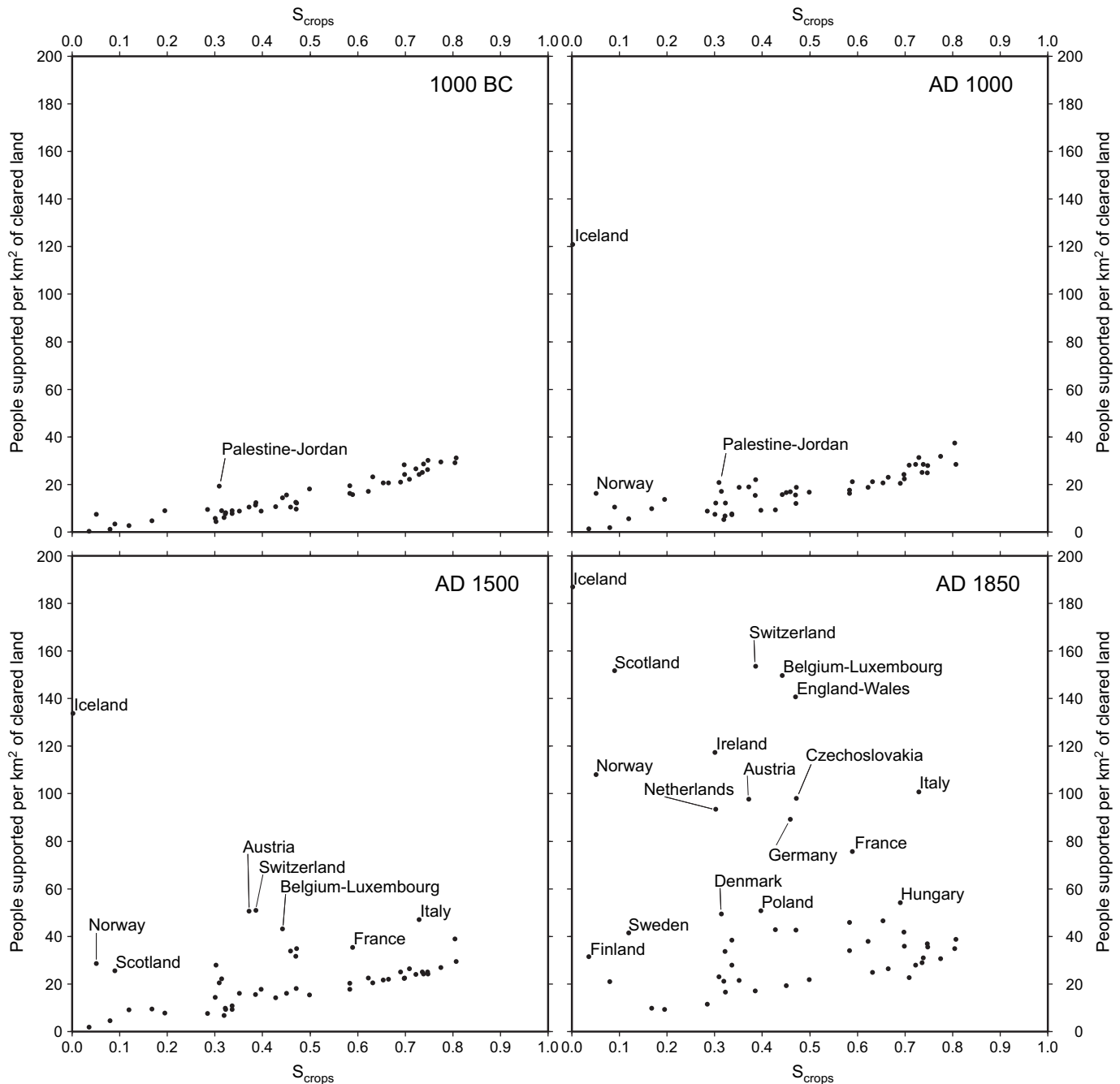
Fig. 9. People supported per km² of cleared land at 1000 BC, AD 1000, AD 1500, and AD 1850, with each dot representing a population region in our study area. Population regions diverging from the original relationship clearly seen at 1000 BC are labeled.

variable, S_{usable}, was necessary for our purposes of estimating total land clearance. Values of S_{usable} provide a reliable approximation of hospitable (usable) lands and aid in assessing the impact of various kinds of human influences on European landscapes such as pasture area or simply area where people can inhabit long enough to clear trees. Furthermore, by comparing the distribution of values for S_{crops} and S_{usable}, it is evident that soil limitations (pH_{soil} and C_{soil}) provide much of the spatial variability in our model. Lands with a high S_{crops}, and therefore lands having neutral pH and moderate carbon density, are allocated as agricultural areas first. This assumption is reasonable because humans can adequately observe soil quality and an agricultural society would likely have understood the advantages of farming on quality land.

Because S_{usable} is only constrained by climate variables, the mid-latitudes of Europe show consistently high S_{usable}. However, high mountain regions such as the Alps are deemed unsuitable for pastureland. This is a limitation of our model, as summertime pasturing of livestock in mountain areas (transhumance) is common in these areas (Arnold and Greenfield, 2006). Another limitation of the land suitability for crop and pasture dataset can be seen in North Africa and some Near East regions, where suitability is very low due to lack of water. A few major rivers (Nile, Tigris-Euphrates) in these regions allow large populations to be supported by irrigation (Helbaek, 1960; Weiss et al., 1993; Mazoyer and Roudart, 2006), while oases support widespread extensive pasturing in semi-desert areas (Potts, 1993). These limitations lead

to an underestimate of the area of usable land in our model; however, because most of these arid landscapes are not naturally occupied by forest vegetation, they are unlikely to affect our simulations of changes in forest cover.

4.2. Historical forest cover estimates for the standard scenario

Continental-scale syntheses of paleoecological and archaeological data currently do not have sufficient spatial and temporal resolution to make a quantitative data-based evaluation of our model results (Gaillard et al., 2000; Gaillard, 2007; Hellman et al., 2008). We can, however, qualitatively assess our simulations in the context of historical observations. At the beginning of our time domain, our model calculated significant amounts of forest clearance by 1000 BC in the Near East regions of Iraq, Syria-Lebanon, and Palestine-Jordan, all of which lie within the areas of the earliest known permanent agricultural societies, where farming and animal domestication originated more than 6000 years earlier (Ammerman and Cavalli-Sforza, 1971; Cavalli-Sforza, 1996; Bar-Yosef, 1998; Diamond, 2002). Ancient civilizations in this area were larger than in other regions during this time due to the increased food supply from well-established agricultural practices. As mentioned above, the civilizations that were situated around the Euphrates and Tigris rivers used irrigation to extend their usable land into drier areas (Weiss et al., 1993) an aspect of LCLUC that is not captured by our model.

In general, western and central Europe was minimally deforested at 1000 BC according to the standard scenario (Fig. 6). This result is consistent with other estimates of anthropogenic land use at this time (Berglund, 2006). Alpine Europe and Belgium–Luxembourg do show substantial deforestation at this time however, as a result of these regions' high population densities on usable land. Nascent urbanization in Belgium–Luxembourg, and possibly an underestimation of usable land in the Alpine countries – we were unable to account for populations subsisting on transhumance in this model – may mean that our model somewhat overestimates the amount of land cleared in these regions (see also Section 4.1). Several hundred years later, by 300 BC, well-established agriculture and the rise of classical civilizations led to increases in populations and significant deforestation throughout central and western Europe (Fig. 6, year 300 BC). By 200 BC we calculate that population densities exceeded 19 inhabitants per km^2 in Italy and between 10 and 18 inhabitants per km^2 in the rest of Western Europe and Greece. Considering that the carrying capacity of pre-Neolithic (hunter-gatherer) societies and preindustrial agricultural societies is estimated at 0.1 and 15–20 inhabitants per km^2, respectively (Hillman, 1973; McEvedy and Jones, 1978; Clark, 1991), it is reasonable to assume that well-established agriculture, and therefore widespread deforestation, must have been in place during this period to support such numbers of people.

Several regions of North Africa, including Algeria and Tunisia, show particularly high population sizes relative to their land suitability for agriculture and display high amounts of deforestation by 300 BC. By 1000 BC, numerous Phoenician colonies were concentrated in the area of present day Tunisia along the Mediterranean trade routes (McEvedy, 2002). The Carthaginian Empire had reached nearly its greatest power and extent by 300 BC, and high population densities in North Africa would probably have led to widespread deforestation. In Morocco, people were more dispersed given the higher percentage of usable land available in this region compared to other Maghreb regions (Table 3).

First in Greece (roughly 1000 BC to 300 BC) and several centuries later in Italy (roughly 300 BC to AD 200), the Classical Greek and Roman civilizations left their mark on the landscape, depicted in our model as high forest clearance within these regions during these periods. Williams (2000) provides recorded descriptions of extensive deforestation in these regions by Greek author Homer (9th century BC) and Roman author Lucretius (1st century BC), thus qualitatively verifying our model results. The fall of both the Greek and Roman empires were marked by periods of afforestation, as populations declined and land was abandoned (Table 3). Because the Roman Empire was particularly widespread throughout Europe we simulate a slight rise in deforestation throughout Europe (except for some parts of Eastern Europe) through the forth century AD (Fig. 8, all groups; Table 3). This point marked the onset of the collapse of the Roman Empire, the beginning of the Migration Period, and the transition to medieval times. During the period from AD 400 to roughly AD 750, war, plagues, invasions from the East, and climate deterioration (Wanner et al., 2008) resulted in stagnating or declining populations across much of Europe. In most regions of Europe, this period is marked by stable forest cover or afforestation.

The next gradual decline in forest cover coincides with the development of feudal societies that provided some political structure, the emergence of western European nation states in Spain, France and England by the 11th century, the establishment of cities across Europe, and climatic amelioration that marked the end of the Migration Period (Wanner et al., 2008). In our model simulations, this expansion is marked by a period of extensive deforestation in central and western European regions (Fig. 6, AD 1000). For example, establishment of a stable and sophisticated government in England after the 11th century Norman Conquest led to deforestation on a large scale, which is recorded in the Domesday Book (Rackham and Rackham, 1994).

Eastern Europe, which showed lower levels of deforestation than did most other regions in our study area, was subject to political and cultural unrest during the medieval period. Dominated by the Bulgarian Empire until just after the onset of the 11th century, Eastern Europe was then invaded by eastward-migrating Germanic peoples heading to less densely-populated lands (Darby, 1956; Williams, 2000). This observation from the historical record provides additional evidence that the landscapes of Western Europe were nearing their carrying capacity by this time, given their relatively limited technological sophistication. Lastly, certain regions of Eastern Europe, particularly the forest-steppes of Russia, Romania and Hungary, rich in cultivatable land, were conquered by successive waves of westward-migrating peoples of central Asian origin during medieval times, and became part of the Mongolian Empire for several centuries.

In all of these cases throughout Europe, forest cover retreated as populations became denser and societies advanced. This retreat in forest cover during the 11th–13th centuries, referred to as *l'âge des grands défrichements* (Williams, 2003), was revealed in our model as all regions showed an increase in deforestation (Fig. 8, standard scenario). The Black Death ended this era by devastating the populations of Europe and halting deforestation (Darby, 1956; Williams, 2000). When the populations of Europe recovered 100 years later, the Renaissance and later the Ages of Discovery and Enlightenment brought about an advancement of ideas, science, trade, and religion throughout all of Europe. Even given the disastrous consequences of the 30 Years' War, this period leading up to the Industrial Revolution is expressed in our dataset as a generally uniform decrease in forest cover throughout Europe.

4.3. Uncertainties in population estimates

Since the outcome of our preindustrial anthropogenic deforestation model is heavily based on historical population estimates, any uncertainties associated with this data can strongly influence our

results. The principle population dataset used in this study (McEvedy and Jones, 1978) is generally listed as the lower limit of world population estimates for earlier times (U.S. Census Bureau, 2008) and does not differ greatly from the other two population references that were used. Thus, similar deforestation levels are achieved when running the model with upper- and lowerbound population estimates (Fig. 8, gray area).

Dearing (2006) highlighted the order of magnitude differences between worldwide totals of human population based on the references used in this study (see also U.S. Census Bureau, 2008) and world population estimates generated by a model based on resources, technology and cultural characteristics of Neolithic societies at 1000 BC (Wirtz and Lemmen, 2003). Running our model with upper-limit population estimates for our study region as generated by this model would be an interesting addition to this research.

4.4. Intensification, innovation and technological advancement

The nonlinear relationship between population density and forest cover (Eq. (1)) used in the standard scenario implies a degree of in situ intensification, where, as population densities increase, people invent methods or technologies to maintain more people on the same amount of cleared land (Fig. 3b,c). Though this curve represents some degree of agricultural intensification, it probably underestimates the sometimes-dramatic effect that development of new technologies had on increasing the number of people who could be supported by a landscape. By interpolating the changing shape parameters of our population-forest cover relationship smoothly through time (Fig. 4), our technological change scenario implies continuous improvement over time, albeit at different rates before and after each time slice. Thus, our model of technological advancement follows the view of Boserup (1965), that intensification is a continuous process. At the other extreme, innovation in prehistoric and preindustrial societies might rather have followed a Malthusian pattern, with periods of innovation only occurring in response to resource crises (Malthus, 1798). Whatever the cause, by adding technological advancement to our model, we are able to provide an alternative view of the time series of deforestation that may have taken place over the past 3000 years.

Ammerman and Cavalli-Sforza (1984) estimated that in Europe and the Near East, early farming techniques spread at a rate of 1 km per year from southeast to northwest and had reached even the farthest coasts of Europe by 3000 BC. After the initial occupation of Europe by farming cultures, higher population densities and efficient trade routes throughout Europe would have spread new agricultural advancements relatively quickly. Trade routes, well-established after 1000 BC (Cleland, 1927; McEvedy, 2002), population growth, technological innovations, warfare and colonization favor geographical expansion and thus the exchange of ideas (Cavalli-Sforza, 1996; Wirtz and Lemmen, 2003). The existence of long-distance trade routes in prehistoric Europe is supported by numerous archaeological finds of natural materials (metals, amber, marine items) far from their place of origin (Cleland, 1927; Healy and Scarre, 1993) and is illustrated by the discovery of the iceman Ötzi who, at ca. 3200 BC, was traveling on a well-established route through the Alps (Müller et al., 2003). 4500 years later, the Black Death spread across nearly our entire study domain within two years (McEvedy and Jones, 1978), a feat that only could have occurred through frequent and intensive contact between centers of high population density over distances of several thousand kilometers.

Though technological developments could have spread quickly throughout Europe, social, political, and economic differences between cultures meant that the adoption of new technologies was probably uneven in space and time. Dumond (1965) illustrates how innovations such as the mouldboard plow, three-field rotation, or

horse drawn power took several centuries to be widely used in western Europe alone. Some regions in our spatial domain, such as parts of interior Anatolia, used essentially medieval farming techniques as late as the mid-20th century (Hillman, 1973). Furthermore, the forest transition, commonly driven by a certain level of economic and social development (Rudel et al., 2005), occurred ca. 100 years later in the Carpathian mountain range than in the Alps (Mather, 1999; Mather and Fairbairn, 2000; Kozak et al., 2007). Thus, without considering these differences, deforestation in our technology scenario could have been underestimated in some regions and our technology scenario should be viewed as an upper bound estimate of the potential effects of technological change over our spatial and temporal domains. The political, cultural, and economic differences between regions are further exemplified when synthesizing graphs of land quality vs. people supported per area of cleared land.

4.5. People supported per km^2 of cleared land

By studying the modeled relationship between land quality (S_{crops}) and population density (Fig. 9) and the time history of this relationship, we are able to speculate on the carrying capacity and long-term sustainability of agriculture on European landscapes. In general, higher quality arable land is able to support greater population densities. At low levels of technological sophistication (Fig. 9, 1000 BC time slice), the positive linear relationship is clear for nearly all countries. With time, an increasing number of population regions depart from this general trend and tell us something about the unique histories of intensification, technological development, trade, and exploitation of natural resources experienced by each region.

Already at 1000 BC, Palestine-Jordan diverges from the other regions, possibly due to the very long history of agriculture, urbanization, and specialization of labor in this region. While not included in this study, other centers of antiquity such as ancient Egypt would probably show an even greater departure from the initial relationship, where both irrigation and the development of complex civilization contributed to this society's ability to support very high population densities. The outlier regions in the remainder of the time slices presented in Fig. 9 are distinct due to one or more of four trends that enabled these areas to support high population densities. The earliest clear trend is seen in regions that could exploit a marine resource, followed by nascent industrialization and urbanization, international trade, and technological development, all of which were established by the Renaissance.

In AD 1000, regions with a relative paucity of quality agricultural land, such as Norway and Iceland, were able to support large populations through fishing. By the 16th century, Belgium–Luxembourg had developed a sophisticated urbanized population reliant on manufacturing and international trade. Likewise, Switzerland and Austria benefited from their position astride the Alpine passes taking advantage of international trade, while countries along the Mediterranean basin, such as France and Italy, had developed sophisticated agricultural technology and a variety of crops in situ, that only later spread to the rest of Europe (DuPlessis, 1997). In contrast, as time progresses, Palestine-Jordan does not change its position in the relationship. This is consistent with the gradual decline in population and land use intensity in these regions, which may have been partly a result of the preceding millennia of ultimately unsustainable land use (Cordova, 2005). Over-exploitation of the land base even before 1000 BC may have also led to stagnant populations in Iraq and Syria-Lebanon and resulted in a consistently low number of people supported per unit area of cleared land for the entire time domain of our study.

By AD 1850, Belgium–Luxembourg, England–WalesWales, Scotland, Ireland, Austria, the Netherlands, Italy, Germany, France, Switzerland, and Czechoslovakia rank among the highest in terms of people supported per km^2 of cleared land. These countries, with intermediate values of S_{crops} ranging from roughly 0.3 to 0.7, were among the first in Europe to develop very intensive agriculture based on new crops such as the potato, and to embrace the Industrial Revolution. International trade, exploitation of overseas colonies, urbanization, and technological development all contributed to the ability of these regions to support very dense populations independent of their own suitability for agricultural production.

Regions exhibiting little or no change by AD 1850 in the land quality-population density relationship depicted in Fig. 9 not only include the Near East regions mentioned above, but also the North African regions and most of the Eastern European regions (including the regions of European Russia). Eastern European regions are generally characterized by a high degree of land suitability for crops and pasture, thus might not have experienced the population pressure necessary to inspire intensification. Furthermore, the Industrial Revolution and many of the agricultural improvements and trade experienced by the central and western European regions had not yet arrived in Eastern Europe by AD 1850.

### 4.6. The end of the population density – forest cover relationship

The increasing amount of scatter in the land quality-population density relationship towards AD 1850 (Fig. 9) indicates that the simple forest cover-population density relationship used in our model would not be appropriate for later times in history. Many factors that accompany industrialization such as trade, technology, and efficient transportation methods complicate any predictive measures taken to assess historical deforestation by means of population density. Additionally, many regions of Europe started to experience forest transitions by the mid-19th century (Mather, 1992; Mather et al., 1998a), where forest cover and population become uncoupled and the trend is reversed in some cases. Fortunately, there are better historical records of forest cover and reliable datasets of LCLUC after industrialization (Ramankutty and Foley, 1999; Klein Goldewijk, 2001).

4.7. Comparison to other preindustrial LCLUC estimates

Deforestation estimates for AD 1800 in both our standard and technological scenarios are much higher than those in the HYDE dataset (Klein Goldewijk, 2001) (Fig. 10), or in the recent study by recent study by Pongratz et al. (2008). The early 19th century is a low point in forest cover in several western European countries according to all syntheses of historical observations that were available to us (Mather et al., 1998a; Mather, 1999; Mather and Fairbairn, 2000; Bradshaw, 2004), yet at AD 1800, the HYDE dataset estimates European gridcells to be roughly 10%–50% deforested. This result seems unrealistic when compared to the scenarios presented in this study, in which most gridcells are designated as 60%–100% cleared at AD 1800, more in accordance to the forest cover data available. Furthermore, AD 1800 is right before the onset of industrialization, when many forest transitions begin to take place (Rudel et al., 2005), and therefore a period when European countries would have been highly deforested. The HYDE dataset shows continually decreasing forest cover from AD 1800 well into the 20th century, a period when forest cover was actually increasing in several European countries (Mather et al., 1998a,b; Mather, 1999; Mather and Fairbairn, 2000), illustrating that the HYDE dataset is missing some integral components of European forest history. Our dataset also contains much higher estimates of deforestation in medieval times than those presented in Pongratz et al. (2008) (Fig. S1). For example, at AD 1000 both our standard and technological scenarios depict many parts of Europe to be only 10%–20% forested, while Pongratz et al. (2008) depict a highly forested Europe (60%–100% forest cover). The simplistic approaches to scaling anthropogenic land use to total population used in both the HYDE and the Pongratz et al. datasets appear to omit the strongly nonlinear relationship between population and land cover supported by the evidence presented in this study. As shown in our technology scenarios, accounting for the time-dependent development and spread of technology would further exacerbate the mismatch between our results and these earlier studies.

4.8. Model limitations and future directions

We acknowledge several limitations of our deforestation model. First, our model presumes that the primary reason for deforestation
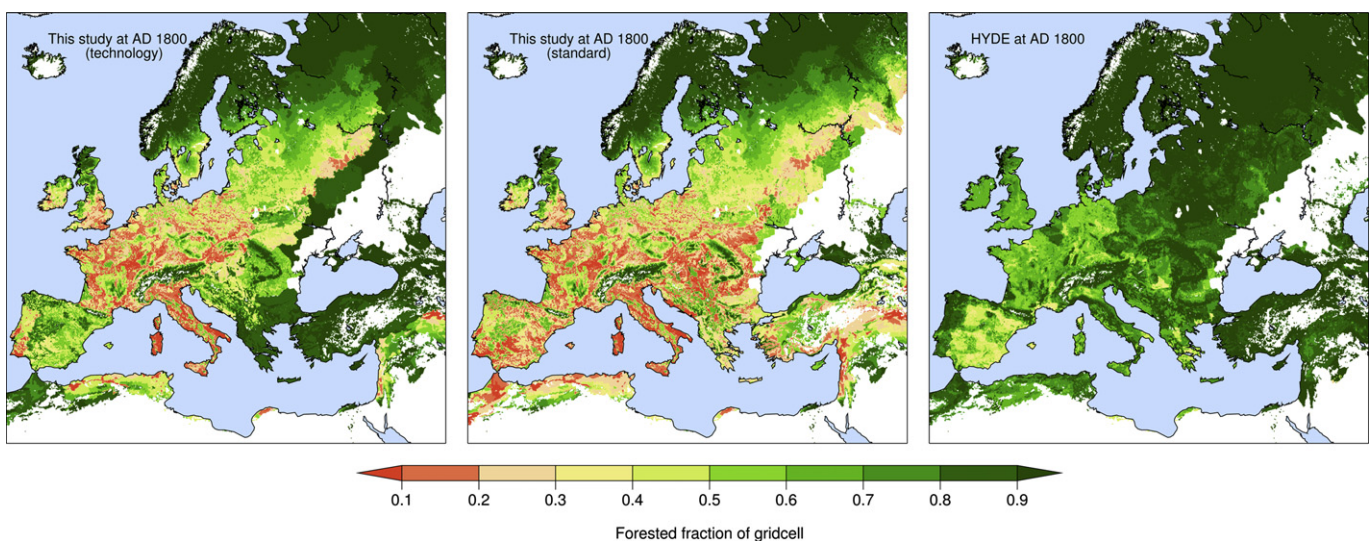
Fig. 10. Comparison of forest clearance maps at AD 1800 as generated by the technological scenario and standard scenario of the preindustrial anthropogenic deforestation model in this study, and the map generated by the HYDE study of areas under crop and pasture (Klein Goldewijk, 2001).

in any given region is the clearing of land for agriculture. However, forests can be cut for many other reasons, such as acquiring wood for building and fuel. For instance, it is known that Scotland was significantly deforested long before industrialization (Smout, 1997; Mather, 2004), but this is not well reflected by our model, which estimates it as only about 27% cleared by the end of our model run. The gridded variable S_{usable}, used in our model, represents land that is "usable" and could have accounted for some of these additional reasons for clearing, but it is impossible to account for all of them, particularly when material flows are inter-regional in scope, e.g., export of timber for construction materials.

Secondly, our model implies that for the entire temporal domain of our study, human population was supported entirely by agriculture. As we noted in the discussion of Fig. 9, this was probably not the case in an increasing number of population regions with time. Human population densities in any given region at any given time were influenced by three major factors independent of deforestation: 1) the ability to a support population by exploiting natural resources, especially through fishing, 2) reliance on inter-regional trade to supply food and other goods, and 3) irrigation, urbanization, and specialization of labor, which allowed in situ intensification to occur. Ultimately it would be useful to include these potential food sources in our model, as well as changes in the nutritional density of crops grown in space and time using historical yield data (e.g., Slicher van Bath, 1963). Furthermore, we assume in our technology scenario that new technologies are adopted simultaneously across our study domain, while it is well known that the diverse political, cultural, and environmental histories of Europe's regions led to an uneven adoption of technology in space and time over the past three millennia. All of these factors probably lead to regional over- and underestimates of deforestation in Europe for the time domain of our study. For example, some of the most fertile regions of Europe were not widely exploited until very recently because of the lack of appropriate agricultural technology. The development of heavy steel plows opened the chernozem regions of Ukrainian and Russian steppe and forest-steppe to intensive agriculture only in the 19th century. To improve our methodology, we would need time-dependent maps of agricultural "potential" based on regionally available technology. Future work on this topic should include spatially explicit chronologies of intensification and technological development based on the historical and archaeological record.

The next logical step for this study would be to extend both our spatial and temporal domains, to cover the globe and the entire Holocene, though issues such as data availability, nutritional/technological heterogeneity and climatic change will have to be overcome. Many other areas of the world experienced an intense anthropogenic impact during the Holocene, including India, China, and parts of South and Central America (Nevle and Bird, 2008). Furthermore, addressing some of the model limitations described above, including focusing on the cultural differences between regions might aid in producing a more accurate estimation of deforestation over the past 3000 years and more. It should also be possible to perform a much more thorough evaluation of our model results through comparison with continental-scale syntheses of paleoecological and archaeological data. While there are many challenges associated with reconciling site-specific observations to gridded model results, new methods for data synthesis (Davis et al., 2003) and model-data comparison make this feasible in the coming years. New tools for landscape reconstruction that make direct use of the paleoecological record, such as the REVEALS model (Sugita, 2007a,b; Hellman et al., 2008), may make it possible to evaluate the deforestation estimates presented in this study for specific regions where these analyses have been performed.

5. Conclusions

This paper describes a novel method for estimating anthropogenic deforestation for preindustrial times. Our methodology is particularly unique compared to other attempts (Ramankutty and Foley, 1999; Klein Goldewijk, 2001; Pongratz et al., 2008) because we used land suitability to crop and pasture to create spatial variability within population regions, minimizing the propagation of errors associated with projecting population density or agricultural areas maps back in time. Our time domain extends back to 1000 BC, late enough to ensure that well-settled agriculture had spread all over Europe, yet early enough to capture some of the prehistoric anthropogenic perturbation of the global carbon cycle, and possibly climate patterns. Our model predicts much greater areas of deforestation as compared to other studies, in both the recent and distant past, but our data is supported by historical observations. Further evaluation of our model results should be done through comparison to paleoecological and archaeological data syntheses. By extending our methodology to a global analysis and applying a terrestrial carbon cycle model, it is conceivable that our model would support Ruddiman's hypothesis that humans have had a substantial influence on the climate system since the mid-Holocene (Ruddiman, 2003, 2005, 2007).

Acknowledgements

Appendix. Supplementary information

Supplementary data associated with this article can be found in the online version at doi:10.1016/j.quascirev.2009.09.028

References

Ammerman, A.J., Cavalli-Sforza, L.L., 1971. Measuring the rate of spread of early farming in Europe. Man 6 (4), 674–688.
Ammerman, A.J., Cavalli-Sforza, L.L., 1984. The Neolithic Transition and the Genetics of Populations. Princeton University Press, Princeton.
Annoni, A., 2005. European Reference Grids: Proposal for a European Grid Coding System. European Commission Joint Research Centre.
Annoni, A., Luzet, C., Gubler, E., Ihde, J., 2001. Map Projections for Europe. European Commission Joint Research Centre.
Arnold, E.R., Greenfield, H.J., 2006. The Origins of Transhumant Pastoralism in Temperate Southeastern Europe: a Zooarchaeological Perspective from the Central Balkans. Archaeopress, Oxford.
Bar-Yosef, O., 1998. The Natufian Culture in the Levant, threshold to the origins of agriculture. Evolutionary Anthropology, 159–176.
Behre, K.-E., 1988. The role of man in European vegetation history. In: Huntley, B., Webb, T. (Eds.), Vegetation History. Kluwer, Dordrecht, pp. 633–672.
Berglund, B.E., 2000. The Ystad Project - A case study of multidisciplinary research on long-term human impact. PAGES Newsletter 8 (3), 6–7.
Berglund, B.E., 2006. Agrarian landscape development in northwestern Europe since the neolithic: cultural and climatic factors behind a regional/continental pattern. In: Hornburg, A., Crumley, C.L. (Eds.), The World System and the Earth System: Global Socioenvironmental Change and Sustainability since the Neolithic. Left Coast Press, Walnut Creek, California, USA.
Bintliff, J.L., 1993. Forest cover, agricultural intensity and population density in Roman imperial Boeotia, central Greece. In: Frenzel, B. (Ed.), Evaluation of Land Surfaces Cleared from Forests in the Mediterranean Region During the Time of the Roman Empire. Fischer Verlag, Stuttgart, pp. 133–143.
Biraben, J.N., 1979. Essai sur L'évolution du nombre des hommes. Population 34 (1), 13–25.
Boserup, E., 1965. The Conditions of Agricultural Growth: the Economics of Agrarian Change Under Population Pressure. Aldine.

Bradshaw, R.H.W., 2004. Past anthropogenic influence on European forests and some possible genetic consequences. Forest Ecology and Management 197, 203–212.

Brewer, S., Williams, J.W., Tarasov, P., Davis, B.A.S., 2008. Changes in European tree cover during the Holocene based on pollen and AVHRR data. Terra Nostra 2, 37–38.

Cavalli-Sforza, L.L., 1996. The spread of agriculture and nomadic pastoralism: insights from genetics, linguistics, and archaeology. In: Harris, D.R. (Ed.), The Origins and Spread of Agriculture and Pastoralism in Eurasia. UCL Press, London, pp. 51–69.

Clark, C., 1977. Population Growth and Land Use. The Macmillan Press Ltd, London.

Clark, G., 1991. Yields per acre in English agriculture, 1250–1860: evidence from labour inputs. Economic History Review XLIV, 445–460.

Clark, P.J., Merkt, J., Müller, H., 1989. Post-glacial fire, vegetation, and human history on the Northern alpine forelands, South-Western Germany. Journal of Ecology 77, 897–925.

Cleland, H.F., 1927. Commerce and trade routes in prehistoric Europe. Economic Geography 3 (2), 232–238.

Cordova, C.E., 2005. The degradation of the ancient near eastern environment. In: Snell, D.C. (Ed.), A Companion to the Ancient Near East. Blackwell Publishing Ltd, Oxford.

Cordova, C.E., Lehman, P.H., 2005. Holocene environmental change in south-western Crimea (Ukraine) in pollen and soil records. The Holocene 2, 263–277.

Darby, H.C., 1956. The clearing of the woodland in Europe. In: Thomas Jr., W.L. (Ed.), Man's Role in Changing the Face of the Earth. University of Chicago Press.

Davis, B.A.S., Brewer, S., Stevenson, A.C., Guiot, J., 2003. The temperature of Europe during the Holocene reconstructed from pollen data. Quaternary Science Reviews 22, 1701–1716.

Dearing, J.A., 2006. Climate-human-environment interactions: resolving our past. Climate of the Past 2, 187–203.

DeFries, R.S., Field, C.B., Fung, I., Collatz, G.J., Bounoua, L., 1999. Combining satellite data and biogeochemical models to estimate global effects of human-induced land cover change on carbon emissions and primary productivity. Global Biogeochemical Cycles 13 (3), 803–815.

Diamond, J., 2002. Evolution, consequenes and future of plant and animal domestication. Nature 418, 700–707.

Dümenil Gates, L., Ließ, S., 2001. Impacts of deforestation and afforestation in the Mediterranean region as simulated by the MPI atmospheric GCM. Global and Planetary Change 30, 309–328.

Dumond, D.E., 1965. Population growth and cultural change. Southwestern Journal of Anthropology 21 (4), 302–324.

DuPlessis, R.S., 1997. Agriculture: growth and limits of development. In: DuPlessis, R.S. (Ed.), Transitions to Capitalism in Early Modern Europe. Cambridge University Press, Cambridge.

Eugster, W., Rouse, W.R., Pielke, S.A., McFadden, J.P., Baldocchi, D.D., Kittel, T.G., Chapin, I.F.S., Liston, G.E., Vidale, P.L., Vaganov, E., Chambers, S., 2000. Land-Atmosphere energy exchange in arctic tundra and boreal forest: available data and feedbacks to climate. Global Change Biology 6, 84–115.

FAO/IIASA/ISRIC/ISSCAS/JRC, 2008. Harmonized World Soil Database (Version 1.0). FAO, Rome, Italy and IIASA, Laxenburg, Austria.

Gaillard, M.-J., 2007. Detecting human impact in the pollen record. In: Elias, S.A. (Ed.), Encyclopedia of Quaternary Science. Elsevier, University of London, pp. 2570–2595.

Gaillard, M.-J., Sugita, S., Bröstrom, A., Eklöf, M., Pilesjö, P., 2000. Long term land-cover changes on regional to global scales inferred from fossil pollen – how to meet the challenges of climate research? PAGES Newsletter 8 (3), 30–32.

Halsall, G., 2007. Barbarian Migrations and the Roman West: 376–568. Cambridge University Press, Cambridge.

Healy, F., Scarre, C., 1993. Trade and Exchange in Prehistoric Europe. Oxbow Books, Oxford.

Helbaek, H., 1960. Ecological effects of irrigation in ancient Mesopotamia. Iraq 22, 186–196.

Hellman, S.E.V., Gaillard, M.-J., Bröstrom, A., Sugita, S., 2008. Effects of the sampling design and selection of parameter values on pollen-based quantitive reconstructions of regional vegetation: a case study in southern Sweden using the REVEALS model. Vegetation History and Archaeobotany 17, 445–459.

Hijmans, R.J., Cameron, S.E., Parra, J.L., Jones, P.G., Jarvis, A., 2005. Very high resolution interpolated climate surfaces for global land areas. International Journal of Climatology 25, 1965–1978.

Hillman, G., 1973. Agricultural productivity and past population potential at Aşüvan: an exercise in the calculation of carrying capacities. Anatolian Studies 23, 225–240. Aşüvan 1968–1972: An Interim Report.

Hughes, J.D., Thirgood, J., 1982. Deforestation, erosion, and forest management in ancient Greece and Rome. Journal of Forest History 26 (2), 60–75.

Jurkat, K.-P., 2004. Gedanken und Fakten zur Bevölkerungsentwicklung in Ost-preußen. http://www.prussen.org/besiedelung-bevoelkerungsentwicklung-ostpreussen.htm.

Klein Goldewijk, K., 2001. Estimating global land use change over the past 300 years: the HYDE Database. Global Biogeochemical Cycles 15 (2), 417–433.

Kozak, J., Estreguil, C., Troll, M., 2007. Forest cover changes in the northern Carpathians in the 20th century: a slow transition. Journal of Land Use Science 2 (2), 127–146.

Lagerås, P., Jansson, K., Vestbö, A., 1995. Land-use history of the Axlarp area in the Småland uplands, southern Sweden: palaeoecological and archaeological investigations. Vegetation History and Archaeobotany 4, 223–234.

Lewis, R.A., Leasure, J.W., 1966. Regional population changes in Russia and the USSR since 1851. Slavic Review 25, 663–668.

Malthus, T.R., 1798. An Essay on the Principle of Population. Printed for J. Johnson, in St. Paul's Church-yard.

Mather, A.S., 1992. The forest transition. Area 24, 367–379.

Mather, A.S., 1999. The course and drivers of the forest transition: the case of France. Journal of Rural Studies 15 (1), 65–90.

Mather, A.S., 2004. Forest transition theory and the reforesting of Scotland. Scottish Geographical Journal 120 (1), 83–98.

Mather, A.S., Needle, C.L., 2000. The relationships of population and forest trends. The Geographical Journal 166 (1), 2–13.

Mather, A.S., Fairbairn, J., 2000. From floods to reforestation: the forest transition in Switzerland. Environment and History 6, 399–421.

Mather, A.S., Needle, C.L., Coull, J.R., 1998a. From resource crisis to sustainability: the forest transition in Denmark. International Journal of Sustainable Development 5, 182–193.

Mather, A.S., Needle, C.L., Fairbairn, J., 1998b. The human drivers of global land cover change: the case of forests. Hydrological Processes 12, 1983–1994.

Mazoyer, M., Roudart, L., 2006. A History of World Agriculture. Earthscan, London.

McEvedy, C., 2002. The New Penguin Atlas of Ancient History. Penguin Books Ltd., London.

McEvedy, C., Jones, R., 1978. Atlas of World Population History. Penguin Books Ltd., London.

Müller, W., Fricke, H., Halliday, A.N., McCulloch, M.T., Wartho, J.-A., 2003. Origin and migration of the alpine iceman. Science 302, 862–866.

Nevle, R.J., Bird, D.K., 2008. Effects of syn-pandemic fire reduction and reforestation in the tropical Americas on atmospheric CO_2 during European conquest. Palaeogeography, Palaeoclimatology, Palaeoecology 264 (1–2), 25–38.

New, M., Lister, D., Hulme, M., Makin, I., 2002. A high-resolution dataset of surface climate over global land areas. Climate Research 21, 1–25.

Olofsson, J., Hickler, T., 2007. Effects of human land-use on the global carbon cycle during the last 6,000 years. Vegetation History and Archaeobotany 17 (5), 605–615.

Päivinen, R., Lehikoinen, M., Schuck, A., Höme, T., Väätäinen, S., Kennedy, P., Folving, S., 2001. Forest Map of Europe. EFI Research Report 14. European Forest Institute and Joint Research Centre – European Commission.

Pinhasi, R., Fort, J., Ammerman, A.J., 2005. Tracing the origin and spread of agriculture in Europe. PLOS Biology 3 (12), 2220–2228.

Pongratz, J., Reick, C., Raddatz, T., Claussen, M., 2008. A reconstruction of global agricultural areas and land cover for the last millennium. Global Biogeochemical Cycles 22 (GB3018).

Pongratz, J., Reick, C., Raddatz, T., Claussen, M., 2009. Effects of anthropogenic land cover change on the carbon cycle of the last millennium. Global Biogeochemical Cycles 23 (GB4001).

Potts, D.T., 1993. The late prehistoric, protohistoric, and early historic periods in Eastern Arabia (ca. 5000–1200 B.C.). Journal of World Prehistory 7 (2), 163–212.

Prentice, I.C., Sykes, M.T., Cramer, W., 1993. A simulation model for the transient effects of climate change on forest landscapes. Ecological Modelling 65, 51–70.

Price, T.D., 2000. Europe's First Farmers. Cambridge University Press, Cambridge.

R Development Core Team, 2005. R: A Language and Environmental for Statistical Computingm Reference Index 2.2.1. R Foundation for Statistical Computing, Vienna, Austria. ISBN 3-900051-07-0. http://www.R-project.org.

Rackham, O., Rackham, J., 1994. Trees and woodland in Anglo-Saxon England: the documentary evidence. In: Rackham, J. (Ed.), Environment and Economy in Anglo-Saxon England. Council for British Archaeology.

Ramankutty, N., Foley, J.A., 1999. Estimating historical changes in global land cover: croplands from 1700 to 1992. Global Biogeochemical Cycles 13 (4), 997–1027.

Ramankutty, N., Foley, J.A., Norman, J., McSweeney, K., 2002. The global distribution of cultivatable lands: current patterns and sensitivity to possible climate change. Global Ecology and Biogeography 11, 377–392.

Ruddiman, W.F., 2003. The anthropogenic greenhouse era began thousands of years ago. Climatic Change 61, 261–293.

Ruddiman, W.F., 2005. Plows, Plagues, and Petroleum: How Humans Took Control of the Climate. Princeton University Press, Princeton.

Ruddiman, W.F., 2007. The early anthropogenic hypothesis: challenges and responses. Reviews of Geophysics 45 (4). doi:10.1029/2006RG000207.

Ruddiman, W.F., Vavrus, S.J., Kutzbach, J.E., 2004. A test of the overdue-glaciation hypothesis. Quaternary Science Reviews 24, 1–10.

Rudel, T.K., Coomes, O.T., Moran, E., Achard, F., Angelson, A., Xu, J., Lambin, E., 2005. Forest transitions: towards a global understanding of land use change. Global Environmental Change 15, 23–31.

Saxon, K.E., Rawls, W.J., 2006. Soil water characteristic estimates by texture and organic matter for hydrologic solutions. Soil Science Society of America Journal 70, 1569–1578.

Slicher van Bath, B.H., 1963. Yield Ratios, 810–1820. Afdeling Agrarische Geschiedenis Landbouwhogeschool, Wageningen, Netherlands, 264 pp.

Smout, C., 1997. Highland land-use before 1800: misconceptions, evidence and realities. In: Smout, C. (Ed.), Scottish Woodland History. Scottish Cultural Press, Dalkeith.

Sugita, S., 2007a. Theory of quantitative reconstruction of vegetation II: all you need is LOVE. Holocene 17, 243–257.

Sugita, S., 2007b. Theory of quantitative reconstruction of vegetation I: pollen from large sites REVEALS regional vegetation. Holocene 17, 229–241.

U.S. Census Bureau, 2008. Historical Estimates of World Population. http://www.census.gov/ipc/www/worldhis.html.

Vavrus, S., Ruddiman, W.F., Kutzbach, J.E., 2008. Climate model tests of the anthropogenic influence on greenhouse-induced climate change: the role of early human agriculture, industrialization, and vegetation feedbacks. Quaternary Science Reviews 27, 1410–1425.

Vermoere, M., Smets, E., Waelkens, M., Vanhaverbeke, H., Librecht, I., Paulissen, E., Vanhecke, L., 2000. Late Holocene environmental change and the record of human impact at Gravgaz near Sagalassos, southwest Turkey. Journal of Archaeological Science 27 (7), 571–595.

Wanner, H., Beer, J., Bütikofer, J., Crowley, T.J., Cubasch, U., Flückiger, J., Goosse, H., Grosjean, M., Joos, F., Kaplan, J.O., Küttel, M., Müller, S.A., Prentice, I.C., Solomina, O., Stocker, T.F., Tarasov, P., Wagner, M., Widmann, M., 2008. Mid- to Late Holocene climate change: an overview. Quaternary Science Reviews 27, 1791–1828.

Weiss, H., Courty, M.A., Wetterstrom, W., Guichard, F., Senior, L., Meadow, R., Curnow, A., 1993. The Genesis and collapse of third millennium North Mesopotamian civilization. Science 261 (5124), 995–1004.

Williams, M., 2000. Dark ages and dark areas: global deforestation in the deep past. Journal of Historical Geography 26, 28–46.

Williams, M., 2003. Deforesting the Earth: from Prehistory to Global Crisis. University of Chicago Press, Chicago.

Wirtz, K.W., Lemmen, C., 2003. A global dynamic model for the Neolithic transition. Climatic Change 59, 333–367.